

Contents lists available at [ScienceDirect](#)

Journal of Hydrology

journal homepage: www.elsevier.com/locate/jhydrol

Abiotic and biotic factors influencing the mobility of arsenic in groundwater of a through-flow island in the Okavango Delta, Botswana

Natalie Mladenov^{a,*}, Piotr Wolski^{b,c}, Ganga M. Hettiarachchi^d, Michael Murray-Hudson^c, Hersy Enriquez^a, Sivaramakrishna Damaraju^a, Madhubhashini B. Galkaduwa^d, Diane M. McKnight^e, Wellington Masamba^c

^a Department of Civil Engineering, Kansas State University, Manhattan, KS, USA

^b Climate System Analysis Group, University of Cape Town, South Africa

^c Okavango Research Institute, University of Botswana, Maun, Botswana

^d Department of Agronomy, Kansas State University, Manhattan, KS, USA

^e Department of Civil, Environmental, and Architectural Engineering, INSTAAR, University of Colorado, Boulder, CO, USA

ARTICLE INFO

Article history:
Available online xxxxx

Keywords:
Arsenic
Sulfate reduction
Iron
Evapoconcentration
DOC
Africa

SUMMARY

The Okavango Delta of Botswana is a large arid-zone wetland comprising 20,000 km² of permanent and seasonal floodplains and over 100,000 islands. It has been shown that island groundwater can have very high dissolved arsenic (As) concentration, but the abiotic and biotic controls on As mobility are not well understood in this setting. At New Island, an island located in the seasonal swamp, dissolved As concentration increased from below detection limits in the surface water to 180 µg/L in groundwater, present as As(III) species. We investigated the relative importance of hydrologic, geochemical, and geomicrobial processes, as well as influences of recent extreme flooding events, in mobilizing and sequestering As in the shallow groundwater system under this island. Our results suggest that evapotranspiration and through-flow conditions control the location of the high arsenic zone. A combination of processes is hypothesized to control elevated As in the concentration zone of New Island: high evapotranspiration rates concentrate As and other solutes, more alkaline pH leads to desorption of arsenic or dissolution of arsenic sulfides, and formation of thioarsenic complexes acts to keep arsenic in solution. Evidence from X-ray absorption near-edge structure spectroscopy (XANES) and sulfate reducing bacteria (SRB) measurements further suggests that SRBs influence arsenic sequestration as orpiment (As₂S₃). Although dissolved organic matter (DOM) was not significantly correlated to dissolved As in the groundwater, our results suggest that DOM may serve as an electron donor for sulfate reduction or other microbial reactions that influence redox state and As mobility. These results have important implications for water management in the region and in other large wetland environments. The processes evaluated in this study are also relevant for arsenic removal in subsurface constructed wetland systems that may exhibit rapidly changing processes over small spatial scales.

© 2013 Published by Elsevier B.V.

1. Introduction

The occurrence of arsenic in groundwater of the Okavango Delta of Botswana is presently one of only several known cases of geogenic arsenic contamination on the African continent (Huntsman-Mapila et al., 2006, 2011; Ravenscroft et al., 2009).

* Corresponding author. Address: Department of Civil Engineering, Kansas State University, 2118 Fiedler Hall, Manhattan, KS 66506, USA. Tel.: +1 785 532 0885; fax: +1 785 532 7717.

E-mail addresses: mladenov@ksu.edu (N. Mladenov), wolski@csag.uct.ac.za (P. Wolski), ganga@ksu.edu (G.M. Hettiarachchi), mmurray-hudson@ori.ub.bw (M. Murray-Hudson), hfenriquez@ksu.edu (H. Enriquez), damaraju@ksu.edu (S. Damaraju), buddhika@k-state.edu (M.B. Galkaduwa), diane.mcknight@colorado.edu (D.M. McKnight), wmasama@ori.ub.bw (W. Masamba).

The Okavango Delta of Botswana is located in an arid zone that includes the Kalahari Desert to the south and Namibia to the west. This 20,000 km² wetland system includes over 100,000 islands, ranging in size from a few meters to over 50,000 ha (Gumbrecht et al., 2004). Elevated arsenic concentrations have been measured in shallow groundwater underlying an island (Camp Island) in the Okavango Delta proper (Huntsman-Mapila et al., 2011) and in deep groundwater (>70 m) southeast of the Okavango Delta, near the town of Maun (Huntsman-Mapila et al., 2006). At Camp Island the highest total dissolved As (3.2 mg As L⁻¹) was measured in groundwater of the central part of the island where salinity and conductivity values were also highest (Huntsman-Mapila et al., 2011). Evaporative concentration of As and other solutes in the

high concentration zone at the center of Camp Island was found to be a major driver of elevated As at this site, and the question of whether elevated As is associated with groundwater underlying the barren island centers of other islands has been raised.

The source of arsenic in the Okavango is geogenic but the exact origin has not been confirmed. Arsenic may derive from weathering of granitic bedrock in the headwaters in Angola, which has been proposed by [Huntsman-Mapila et al. \(2006\)](#) or potentially may be associated with rift tectonics. The tectonically-active Okavango Delta is the southwestern branch of the East African Rift Valley ([Milzow et al., 2009](#)). In the Main Ethiopian Rift sector of the East African Rift Valley, the rhyolitic rocks and their weathered and re-worked fluvio-lacustrine sediments have high content of As, as well as F, Mo, U, and V, and may be the source of these toxic elements elsewhere in the region ([Rango et al., 2010](#)).

The mobilization of geogenic arsenic from sediments in different parts of the world can be described by three main mechanisms. Arsenic can be mobilized under oxidizing conditions that lead to the dissolution of arsenopyrite or sulfidic minerals ([Welch et al., 2000](#); [Schreiber et al., 2000](#)). In a second case, common in arid zones with alkaline, oxidizing groundwater and evapoconcentration of solutes, such as in the southwestern USA, La Pampa, Brazil and elsewhere in the Chaco-pampean aquifer, arsenate desorbs mainly from Fe oxyhydroxides and other mineral oxides at high pH ([Ravenscroft et al., 2009](#)). Finally, perhaps the most widely documented occurrence of groundwater arsenic pollution is in south and southeast Asia, where tens of millions of people have been exposed to arsenic concentrations above the World Health Organization recommended limit of $10 \mu\text{g As L}^{-1}$ ([Mukherjee and Bhattacharya, 2001](#); [Ahmed et al., 2004](#); [Fendorf et al., 2010](#)). In southeast Asia, arsenic is mobilized from sediments mainly as a result of microbial reductive dissolution of Fe- and As-bearing minerals, for which labile dissolved organic matter is the electron donor ([Mukherjee and Bhattacharya, 2001](#); [McArthur et al., 2004](#); [Smedley and Kinniburgh, 2002](#)).

The Okavango Delta comprises two environments where elevated As concentrations are typically found in groundwater, specifically arid-zone closed basin environments and strongly reducing alluvial aquifers ([Smedley and Kinniburgh, 2002](#); [Nordstrom, 2002](#)). The co-existence of both of these environments has been a challenge for identification of the triggers leading to high groundwater As concentration in the Okavango Delta. [Huntsman-Mapila et al. \(2011\)](#) postulated that elevated arsenic in the Okavango Delta may result from a combination of evapoconcentration of dissolved arsenic, possibly released by reductive dissolution earlier along the groundwater flowpath, and desorption of arsenic from sediments at higher pH. In addition, [Huntsman-Mapila et al. \(2011\)](#) identified that redox processes and the influence of DOM and iron on arsenic mobilization needed further investigation.

The presence of elevated arsenic concentrations where arid conditions and reducing sediments coexist is not unique to the Okavango Delta. Elevated arsenic concentrations have also been found in the San Joaquin Delta of California, USA ([Belitz et al., 2003](#); [Izbicki et al., 2008](#)), which has alluvial and fluvial deposits. There, redox conditions are highly variable and elevated As may result from several mechanisms, including reductive dissolution of Fe minerals, evapoconcentration of As, and desorption of As from sediments at high pH ([Belitz et al., 2003](#)).

In wetlands, organic matter is typically a major reservoir for sulfur ([Langner et al., 2011](#)) and, in the event of sulfate depletion, the organic S pool also may be an important source of sulfate upon oxidation of organic material ([Strickland et al., 1987](#)). Under reducing conditions and in the presence of ample amounts of organic carbon as an electron donor, sulfate reducing bacteria (SRB) readily convert sulfate to hydrogen sulfide, which contributes to As(III) removal via the precipitation of As_2S_3 (orpiment) ([Stumm and Morgan, 1996](#);

[Lizama et al., 2011](#)). In evaporation basins of the San Joaquin Valley, California, which are used for the disposal of agricultural drainage, the sediments were a sink for As ([Ryu et al., 2011](#)) and chemical equilibrium modeling suggested that orpiment was formed ([Ryu et al., 2002](#)). In this environment [Gao et al. \(2007\)](#) identified that the potential role of DOM as a complexing agent with sulfide to maintain As in solution warranted further investigation. Indeed, the formation of thioarsenic species has been shown to keep As mobile in a variety of environments, such as sulfidic waters with orpiment dissolution ([Suess and Planer-Friedrich, 2012](#)), mine-impacted groundwater under sulfate-reducing conditions ([Stucker et al., 2013](#)), and geothermal waters ([Planer-Friedrich et al., 2007](#)).

To address some of the gaps in our knowledge regarding arsenic mobility in wetlands influenced by evaporation, the objectives of this study were (1) to characterize the chemical behavior of As along a groundwater flowpath with a natural evaporation gradient and (2) to evaluate the influence of redox processes, microorganisms, and hydrology on dissolved constituents, including DOM and arsenic. These goals also allowed us to test whether elevated As is widely associated with zones of evapoconcentration in groundwater of Okavango Delta islands. We evaluated groundwater solute and sediment chemistry along a west–east transect at New Island, a small island in the seasonal swamp of the Okavango Delta located approximately 20 km downstream of previously-studied Camp Island ([Figs. 1 and 2](#)). This study was conducted at the end of the annual flood season and after several years of intense flooding, which made it possible to also examine the influence of extreme flooding on groundwater biogeochemical processes and As mobility.

2. Methods

2.1. Study site and hydrogeologic setting

The Okavango Delta is located in the northwest of Botswana in southern Africa ([Fig. 1](#)). It is both an alluvial fan and an extensive wetland system that is annually flooded by approximately 10 km^3 of water originating in the Angolan Highlands and delivered via the Okavango River. In this region, evaporation exceeds precipitation by three to four times ([McCarthy and Ellery, 1995](#); [Ramberg and Wolski, 2008](#)). Within the Okavango Delta, the Okavango River diverges into a series of distributary channels and floodplains that carry the water to its distal reaches ([Fig. 1](#)). The Boro River system ([Fig. 1](#)) conducts water through permanently-flooded and seasonally-flooded hydrotones, which have been described elsewhere ([McCarthy and Ellery, 1995](#); [Wolski and Savenije, 2006](#)).

Islands are a characteristic landscape feature in the Okavango Delta. Islands initiate as termite mounds, scrollbars, and inverted channels, and grow as a result of calcite precipitation, dust accumulation, and sedimentation ([Gumbrecht et al., 2004](#)). During the annual flood, surface water replenishes groundwater stores, including those of islands, and evapotranspiration drives the net groundwater flow toward island centers ([McCarthy, 2006](#); [Milzow et al., 2009](#)). The groundwater flow, solute transport, and resulting solute accumulation in groundwater have been described and modeled extensively ([Gieske, 1996](#); [Wolski et al., 2005](#); [McCarthy, 2006](#); [Bauer et al., 2006](#); [Wolski and Savenije, 2006](#); [Bauer-Gottwein et al., 2007](#); [Milzow et al., 2009](#)). Zones of high solute concentration generally occur near the center of islands. Consequently, the ground surface above these zones of solute accumulation is typically barren or colonized only by salt-tolerant vegetation. At New Island, the zone of solute accumulation does not occur at the island center. Instead, a gradient formed by higher water table on the upstream side and lower water table elevation on the downstream side ([Fig. 2](#)) leads to a shifting of the concentration zone toward the eastern beach ([Bauer-Gottwein et al., 2007](#)). Interpolated electrical conductivity

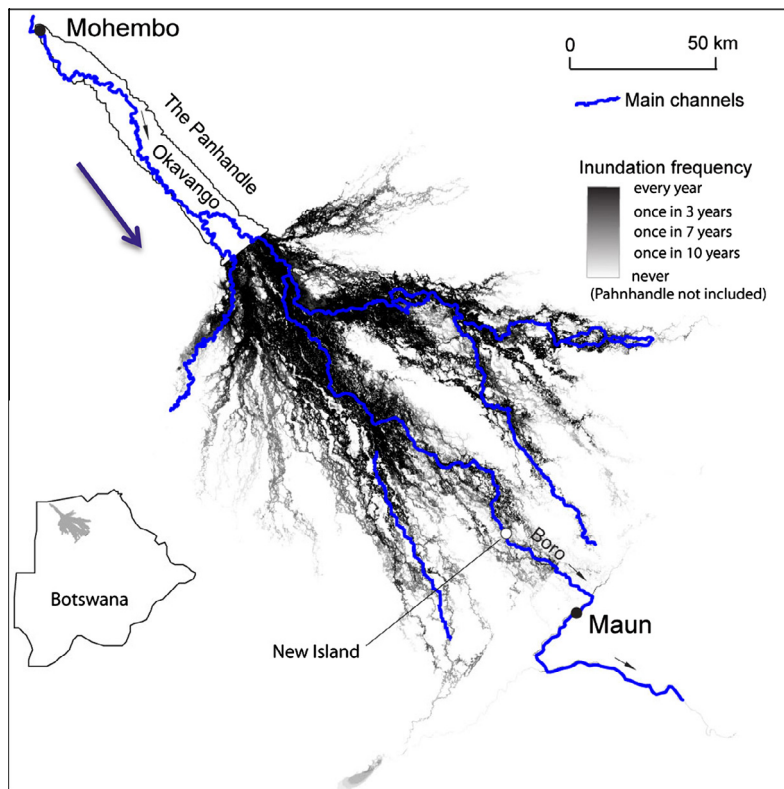


Fig. 1. Map of the Okavango Delta showing the location of New Island, the Boro channel (blue line), and inundation frequency. Arrow shows general direction of surface water flow from northwest to southeast.

and chloride concentration data from 2004 (Bauer-Gottwein et al., 2007) shown in Fig. 2c and d illustrate the accumulation of solutes at New Island near the eastern beach. From our measurements of the seasonal variation of groundwater table elevation, we hypothesize that the shifting of the concentration zone is a function of two-phase flow, dominated by through-flow during flood inundation (May through October) and evapotranspiration-driven concentric flow during the rainy season that follows (Fig. 3).

The accumulation of solutes in groundwater leads to important geochemical reactions, such as precipitation reactions (McCarthy, 2006; Zimmermann et al., 2006), carbon dioxide degassing, and density-driven sinking of dense saline brine (Bauer-Gottwein et al., 2007). Bauer-Gottwein et al. (2007) used geochemical modeling and solute chemistry data collected from three islands in the Okavango Delta, including New Island, to demonstrate that density-driven flow ultimately stabilizes dissolved solids concentrations in island groundwater.

New Island is located in the lower part of the Boro River system and flanks a side channel that is connected to the Boro River (referred to as Boro side channel here; Fig. 2). For the geochemical modeling described above, the groundwater along a west-east transect at New Island was sampled in 2003 by Bauer-Gottwein et al. (2007). For the present study, groundwater and sediments were sampled in October 2011 along the same west-east transect and at similar depths as in the 2007 study (Table 1; Fig. 2). In the austral summer of 2010 and 2011, flood levels throughout the Okavango Delta were higher than they had been in 40 years (Wolski, personal communication).

2.2. In situ measurements and sample collection

At New Island, 50 mm diameter wells were drilled with a hand auger to a depth of between 1.5 m and 2 m at 9 locations along the transect (Table 1; Fig. 2). One well was drilled into an active

termite mound. At two locations, one near the western shore (New 3) and one in the barren eastern beach of the island (New 11), additional wells were drilled to depths of 4 m and 6 m by manual rotary drilling. Prior to sampling, a rinsed PVC pipe fitted with a mesh cover was inserted into each well, and each well was purged 3 times with a peristaltic pump.

Groundwater samples were collected in triplicate after 24 h of well drilling in pre-rinsed and pre-combusted amber bottles. Bottles were filled to overflowing and crimp-sealed immediately. The pH of the groundwater was measured with a Fisher Scientific AP60 pH meter, calibrated with pH 4, pH 7, and pH 10 standards. Electrical conductivity (EC) was measured with a WTW Profiline Cond 3110 meter, calibrated with WIRSAM NR Conductivity Standard solution of 1413 $\mu\text{S}/\text{cm}$ (at 25 °C).

Surface water samples were collected in triplicate in pre-rinsed and pre-combusted amber bottles from approximately 10 cm below the water surface from the channel on the west side of New Island and a floodplain on the east side of the island (Fig. 2).

Sediment samples were collected in air-tight canning jars from sediment recovered during drilling of 2 m, 4 m, and 6 m wells at New 3 and New 11. Jar lids were taped with plumber's tape to further minimize introduction of oxygen.

All surface water, groundwater, and sediment samples were transported on ice to the ORI laboratory within 48 h. One bottle was kept unfiltered as a backup; two bottles were filtered through pre-combusted 0.7 μm nominal pore size glass fiber filters and crimp-sealed inside of a glove bag purged and filled with N_2 gas; one of the filtered bottles was acidified to pH 2 with hydrochloric acid (HCl). All crimp-sealed bottles were transported chilled to the University of Colorado and subsequently kept at 4 °C until analysis. Sediment samples were hand homogenized in the glove bag at ORI and re-packaged in double Zip-lock bags. Sediment samples were shipped chilled to Kansas State University and subsequently kept at 4 °C until analysis.

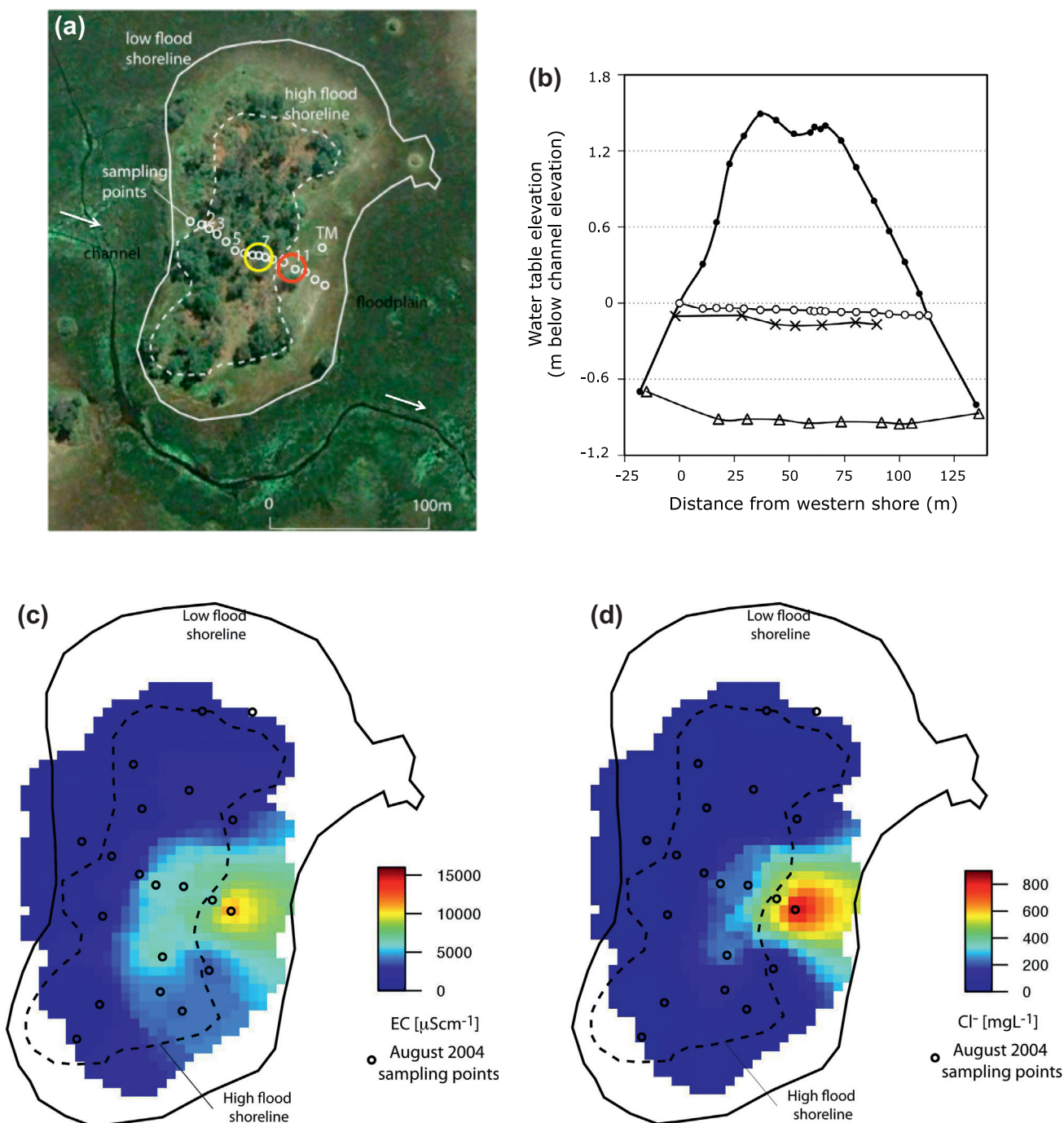


Fig. 2. Plan and profile views of New Island. (a) Aerial photo of New Island showing sampling points (numbered) along a transect parallel to expected groundwater flowpath. New 7 (calcrete zone; yellow circle) and New 11 (the well with the highest As concentration; red circle) are circled. The termite mound (TM) is off the transect. (b) Profile shows water depths measured in August 2004 (x's), October 2011 (circles), and March 2013 (triangles) with exaggerated y-axis to illustrate the higher water level on the west than on the east. Depths and distances are relative to the October 2011 western shore. Maps of (c) electrical conductivity (EC) and (d) chloride concentrations using Bauer-Gottwein et al. (2007) chemical data. Arrows show the direction of flow in Boro side channel.

2.3. Analyses

2.3.1. Water analyses

2.3.1.1. Arsenic speciation. A portion of the filtered-acidified samples were filtered through solid phase extraction (SPE) cartridges (Waters Corporation, Milford, MA). Then SPE-filtered and SPE-unfiltered water samples were analyzed using an Agilent 7500 series inductively coupled plasma-mass spectrometer (ICP-MS) equipped with a dynamic reaction cell. Total As concentration

was directly measured from filtered-acidified (SPE-unfiltered) samples while As (III) concentration was measured from SPE-filtered water samples. Arsenic (V) concentration was calculated from the difference of total As concentration and As (III) concentration (Impellitteri, 2004). For quality control, a NIST standard for trace elements in waters (SRM 1643e) was used and 94% As recovery was achieved with matrix spike recoveries in the range of 90–110%. DRC ICP-MS detection limits for As was below $1 \mu\text{g/L}$ (ppb). Every sample was analyzed in duplicate and relative percent

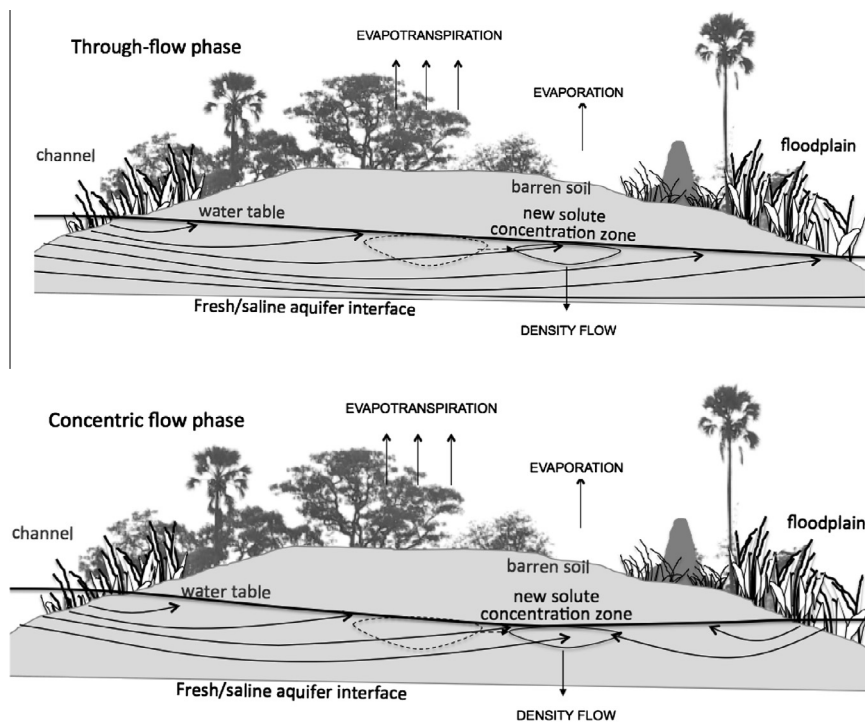


Fig. 3. Conceptual model of groundwater flowpaths during high flood and through-flow conditions (top) and low flood/rainy season and concentric flow conditions (bottom).

differences between duplicated samples were <5% (mostly between 1% and 2%). Analytical blanks and spiked samples were also included and spike recoveries were in the range of 90–110%. Recovery of As in NIST SRM for trace elements in waters (SRM 1643e) was about 94%.

2.3.1.2. Fe^{2+} analysis. An aliquot of a filtered and HCl acidified sample was used for colorimetric determination of soluble Fe^{2+} by the phenanthroline method described by Greenberg et al., 1992 using a Beckman UV-visible DU 800 spectrophotometer. Sample handling and color development were done in the anaerobic N_2 glove box chamber.

2.3.1.3. Total dissolved ion analysis. Total elemental analysis of acidified water samples was done using a Varian 720-ES ICP-optical emission spectrometry (ICP-OES). Prior to measurement with the ICP-OES, samples were filtered through 0.45 μm syringe filters. Unacidified samples were filtered through 0.20 μm syringe filters for the determination of anions. Anions (F^- , Cl^- , NO_2^- , Br^- , NO_3^- , PO_4^{3-} and SO_4^{2-}) were analyzed on an ion chromatograph (IC). Total alkalinity (as $CaCO_3$) was determined in the laboratory by titration with H_2SO_4 .

Dissolved organic carbon (as non-purgeable organic carbon) and total nitrogen concentrations were measured on samples filtered at the ORI laboratory using a Shimadzu TOC-V Total Organic Carbon/Total Nitrogen Analyzer with high salts kit, which includes components designed to reduce clogging of the catalyst in samples with high salt concentrations. Samples were acidified with HCl and sparged for 5 min with ultra-high purity air to remove inorganic carbon.

2.3.1.4. Spectroscopic analyses. UV-vis absorbance and fluorescence of DOM provide optical and chemical information that can be used to describe sources and transformations of DOM. UV-vis absorbance was determined from 200 to 900 nm in a 1-cm path length quartz cuvette using an Agilent 8453 UV-vis spectrophotometer.

UV-vis absorbance was measured in duplicate for each sample. The specific UV absorbance (SUVA), provides information about the aromaticity and chemical reactivity of DOM (Weishaar et al., 2003) and was calculated using Beer's Law as the DOC concentration normalized to the absorbance value at 254 nm, divided by the path length in meters.

Fluorescence spectroscopy provides compositional and chemical information about the fluorescing DOM pool. Excitation emission matrices (EEMs) are a 3-dimensional representation of fluorescence intensities scanned over a range of excitation/emission (ex/em) wavelengths. Prominent humic peaks have been identified, such as in Region A (at ex/em 240–260/380–460 nm) and Region C (at ex/em 320–350/420–480 nm) (Coble, 1996). Peaks at ex/em 275/310 nm and 275/340 nm have been attributed to tyrosine and tryptophan amino acid-like fluorescence (Coble, 1996). Excitation emission matrices were collected with a JY-Horiba Spex Fluoromax-3 spectrophotometer at room temperature using 5 nm excitation and emission slit widths, an integration time of 0.25 s, an excitation range of 240–450 nm at 10 nm increments, and an emission range of 300–560 nm at 2 nm increments. To correct for lamp spectral properties and to compare results with those reported in other studies, spectra were collected in signal-to-reference (S:R) mode with instrument-specific excitation and emission corrections applied during post-processing. Excitation emission matrices were normalized to the Raman area to account for lamp decay over time and to compare with other studies. Raman-normalized ultrapure water blanks were subtracted to remove the Raman scattering signal. Instrument-specific corrections, Raman area normalization, blank subtraction, and generation of EEMs were performed using MATLAB (version R2009b). The two-dimensional fluorescence index (FI) was determined to evaluate microbial and terrestrial contributions to the DOM pool (McKnight et al., 2001). The FI was calculated as the ratio of fluorescence intensities at 470–520 nm for an excitation at 370 nm. After all corrections, EEM spectra are highly reproducible with a standard error for FI of <0.02. The humification index (HIX), used

Table 1
Physical and chemical characteristics of New Island groundwater and adjacent surface water.

Characteristics	New 2	New 3		New 5	New 7	New 9	New 11		New 12	Termite mound	New Island floodplain	Boro side channel
UTM coordinates (zone 34L)	733173	733178		733190	733202	733215	733230		733237	733245	733260	733113
	7821613	7821610		7821597	7821593	7821590	7821583		7821580	7821600	7821560	7821583
Depth of piezometer (m)	2	4	6	2	2	2	4	6	2	2	0	0
Depth of water table (m) ^a	-0.040	-0.041		-0.051	-0.058	-0.071		-0.075	-0.087	-	-0.100	0
Distance (m)	22.70	29.38	29.38	29.38	43.93	59.42	73.53	88.53	88.53	88.53	95.56	100.6 ^a
Conductivity ($\mu\text{S}/\text{cm}$)	2720	826	264	172.3	1630	1876	6520	6610	1410	525	1755	4380
Eh ($\text{As}^{5+}/\text{As}^{3+}$) (V)	0.04			-0.14	-0.14	-0.25	-0.15	-0.02	-0.04	-0.22	-0.09	-0.09
Eh ($\text{NO}_3^-/\text{NO}_2^-$) (V)	0.44	0.46	0.47	0.37	0.36	0.30	0.37	0.43	0.40	0.33	0.41	0.38
pH	7.26	6.62	6.47	6.18	7.99	7.9	8.97	7.8	6.84	7.3	8.53	7.51
$\delta^{18}\text{O}$ (‰)	1.64	3.95	4.45	2.39	4.22	4.01	2.63	2.33	2.82	3.59	2.53	2.75
Stdev $\delta^{18}\text{O}$ (‰)	0.04	0.04	0.02	0.02	0.06	0.04	0.03	0.05	0.04	0.02	0.02	0.03
δD (‰)	-0.54	11.68	13.82	3.38	13.68	13.03	2.79	1.61	4.34	7.15	2.51	3.25
Stdev δD (‰)	0.19	0.12	0.37	0.06	0.28	0.35	0.06	0.09	0.17	0.05	0.13	0.23
Alk (mg CaCO_3/L) ^b	-	750	180	160	1210	-	3900	4520	1050	370	1340	-
F ⁻ (mg/L)	0	0.18	0.39	0.24	0.13	0.16	0.2	0.17	0	0	0.19	0.92
Cl^- (mg/L)	96.6	1.43	2.85	2	6.71	4.1	37.3	39.5	7.4	1.02	1.87	36.8
NO_2^- (mg/L)	1.37	0.33	0.51	0.3	0.62	0.61	0.41	0.41	0.34	0.32	0.29	0.39
Br^- (mg/L)	0	0	0	0	0	0	1.23	1.15	0.99	0	0	0
NO_3^- (mg/L)	16.53	1.2	3.69	1.31	5.57	1.46	1.15	1.12	1.1	1.19	1.71	7.74
PO_4^{3-} (mg/L)	2.03	0	0	0	0	0	0	0	0	0	0	0
SO_4^{2-} (mg/L)	39.1	1.86	2.78	2.36	2.33	1.64	2.66	2.99	2.19	1.69	1.59	8.44
Ca (mg/L)	82.4	51.4	32.5	27.0	78.2	52.2	12.8	16.3	39.6	46.5	28.4	50.6
Mg (mg/L)	27.7	14.6	8.56	4.83	31.9	68.8	17.2	25.6	15.2	7.69	37.0	48.2
Na (mg/L)	216	89.3	12.9	19.6	81.6	82.9	70.8	70.8	80.6	42.5	83.5	71.8
K (mg/L)	191	49.2	14.3	9.79	100	106	360	312	65.1	28.9	124	356
S (mg/L)	14.8	1.80	0.57	0.34	4.58	0.88	6.56	8.45	3.77	1.29	0.25	3.73
Fe (mg/L)	0.33	1.32	3.14	3.44	0.26	0.23	0.10	0.14	0.52	0.90	0.17	0.05
Fe(II) (mg/L)	0.30	1.92	3.62	1.63	0.11	0.11	0.11	0.15	0.58	0.60	0.08	0.13
B (mg/L)	1.31	0.76	0.68	0.68	0.94	0.88	1.10	0.78	0.73	0.76	0.84	1.01
As ($\mu\text{g}/\text{L}$)	33.0	4.26	0.00	0.00	6.22	8.42	97.1	188	17.3	4.01	149	138
As(III) ($\mu\text{g}/\text{L}$)	33.0	2.59	0.00	0.00	5.62	8.16	87.5	186	16.8	2.64	145	129
Se ($\mu\text{g}/\text{L}$)	< 0.5	< 0.5	< 0.5	< 0.5	< 0.5	< 0.5	< 0.5	< 0.5	< 0.5	< 0.5	< 0.5	0
DOC (mg/L)	104	48	32	33	69	52	84	83	35	35	32	62
TDN (mg/L)	11.6	3.01	4.20	0.10	29.7	7.32	4.97	0.10	3.44	2.66	0.10	6.96
SUVA ($\text{L}/\text{mg}/\text{m}$)	1.87	1.99	1.90	1.43	1.43	1.26	1.28	1.64	1.21	1.38	1.03	1.33
UV ₂₅₄ (a.u.) ^c	0.195	0.094	0.062	0.048	0.099	0.065	0.108	0.136	0.042	0.048	0.033	0.083
FI	1.40	1.40	1.51	1.43	1.47	1.51	1.40	1.35	1.50	1.50	1.54	1.51
FI _{max} (nm)	466	466	460	460	462	462	468	464	458	464	462	464
HIX	24.7	15.0	8.0	12.1	15.2	9.3	15.6	23.0	10.6	8.2	6.6	5.3
β/α ratio	0.55	0.52	0.56	0.51	0.57	0.58	0.55	0.52	0.59	0.57	0.59	0.57
SRB (MPN/100 mL)	-	0.0	4.5	4.5	-	-	-	0.0	14	3.7	-	-
Calcite ($\log Q/K$) ^d	-	-0.13	-0.96	-1.37	1.52	-	1.65	0.96	0.09	0.28	1.58	-
Dolomite ($\log Q/K$) ^d	-	0.36	-1.37	-2.35	3.83	-	4.74	3.35	0.93	0.92	4.48	-
Magnesite ($\log Q/K$) ^d	-	-1.14	-2.04	-2.61	0.68	-	1.46	0.76	-0.79	-0.99	1.27	-
Siderite ($\log Q/K$) ^d	-	0.22	-0.13	-0.80	0.39	-	1.06	0.62	0.02	0.17	0.66	-

^a Eh = redox potential; SUVA = specific UV absorbance; FI = fluorescence index; FI_{max} = maximum emission wavelength at 370 nm excitation; UV₂₅₄ = UV absorbance at 254 nm; HIX = humification index; β/α ratio = freshness index; SRB = sulfate reducing bacteria; dash = insufficient sample or sample not collected.

^b Depth relative to Boro side channel.

^c Total alkalinity as mg CaCO_3/L .

^d UV absorbance results shown are for samples diluted 1:10.

^e Modeled saturation indices.

as an indicator of DOM processing and polycondensation, was calculated by using the excitation at 254 nm and dividing the area of emitted fluorescence intensity between 435 and 480 nm by that between 300 and 345 nm (Zsolnay et al., 1999). The freshness index (also called the β/α ratio), used to assess the amount of organic matter recently produced from biological activity, was calculated as the ratio of the β peak (max intensity within ex/em 310–320/380–420 nm) to the α peak (max intensity within ex/em 330–350/420–480 nm) (Parlanti et al., 2000).

2.3.1.5. Sulfate-reducing bacteria (SRB) in groundwater. Sulfate-reducing bacteria were measured using a most probable number technique for water and water-formed deposits according to ASTM D4412-84 (ASTM, 2009). Test tubes with five replicates of three different dilutions were prepared under a sterile environment. The test tubes were sealed with liquid paraffin to maintain anaerobic conditions. Formation of a black precipitate indicated positive reaction of H_2S production.

2.3.2. Sediment sample analyses

Sediment samples were analyzed for As and Fe content after digestion with aqua regia using a ICP-MS (As) or ICP-OES (Fe). The total elemental concentrations in the soils were determined using a 30% H_2O_2 and aqua regia digestion procedure (Bakhtar et al., 1989). Approximately 1 g of soil was predigested with 0.5 mL of H_2O_2 for 10 min at room temperature. Another 2.5 mL of H_2O_2 was added and allowed to react for 12 h at room temperature, after which the tubes were heated on a digestion block at 90 °C until the volume was reduced to ~1 mL. After cooling, the soils were digested using 5 mL of aqua regia (1:3 HNO_3/HCl) using the tube soil digestion procedure (75 °C for 30 min, 100 °C for 30 min, 110 °C for 30 min, and 140 °C until the acid volume decreased to <1 mL), then made up to 20 mL using 0.1% HNO_3 , filtered, and analyzed for total As using DRC ICP-MS and other elements (Al, Si, S, and Fe) using ICP-OES. A standard reference soil (NIST 2711a-Montana II) was also digested in duplicate along with sediment samples as a quality assurance/quality control (QA/QC) sample to evaluate the digestion and analytical procedures. Recovery of As in NIST standard was 80%. The DRC ICP-MS detection limit for As was below 1 $\mu g/L$ (ppb). Every sample was analyzed in duplicate and relative percent differences between duplicated samples were <5% (mostly between 1% and 2%). Analytical blanks and spiked samples were also included and spike recoveries were in the range of 90–110%. Recovery of As in NIST SRM for trace elements in waters (SRM 1643e) was about 94%.

Total carbon (TC), total organic carbon (TOC), and nitrogen content were measured using a Leco CN 2000 combustion analyzer. Cation exchange capacity was determined using the summation method described by Chapman (1965) at pH 7 with 1 M ammonium acetate.

Arsenic K-edge X-ray absorption near-edge structure spectroscopy (XANES) data for selected sediment samples were collected at Sector 5-BMD, Advanced Photon Source (APS), Argonne National Laboratory, IL. The electron storage ring at the APS is operated at 7 GeV with a maximum current of 100 mA. This beamline has an energy range of 4.5–25 keV and is equipped with a Si (III) monochromator with a focused beam size of 1 mm by 1 mm. The sample holder was continuously sprayed with liquid N_2 , and data were collected in fluorescence mode using a Vortex ME4 Silicon Drift Detector. An arsenic filter was used for monochromator calibration. Standards for As included realgar (As_2S_3), orpiment (As_2S_3), elemental As, lollingite ($FeAs_2$), As_2O_3 , As_2O_5 , scorodite ($FeAsO_4 \cdot 2H_2O$), and As^{5+} adsorbed onto ferrihydrite prepared as described in Beak et al. (2006).

The As XANES spectra of a particular sediment sample or a standard was reduced and normalized. The reduced spectrum for the

sample was analyzed by linear combination fitting using IFEFFIT software (Newville, 2001). Mineral saturation states and Nernst Eh values were calculated using the SpecE8 module of The Geochemists Workbench software®, version 9.0.5 (Bethke, 2009). The program used our measured chemical data, the Lawrence Livermore National Laboratory thermodynamic database (Delany and Lundeen, 1990), and an extended form of the Debye–Hückel equation (Helgeson, 1969) to evaluate chemical activities used in the calculations.

2.3.3. Statistical analyses

Bivariate correlations and principal component analysis (PCA) were performed on the original data set (without any weighting or standardization) using the statistical software package STATISTICA 64 (version 9.1). A varimax-normalized rotation was applied to the factor analysis and principal factors with eigenvalues >1.0 were retained.

3. Results

3.1. Groundwater flow and stable isotopes of O and H

Water table elevation of the channel at the west was approximately 100 cm higher than water table elevation of the floodplain to the east of the island (Fig. 2; Table 1). Pressure head was not measured in the piezometers, but groundwater levels declined gradually from west to east. Groundwater beneath New Island had very enriched oxygen and deuterium isotopic signatures and fell along a line that is substantially more influenced by evaporation than the global and local meteoric water lines and more similar to river water from the northwestern Botswana region (Fig. 4). Channel and floodplain surface water isotopes also fell along the groundwater line, with floodplain water to the east of New Island being more enriched than channel water. Isotopic values closer to the shoreline on both sides of the island were more depleted than in the island center (New 5–New 7) and more similar to surface water values (Fig. 4).

3.2. Spatial distribution of solutes

In the surface water, conductivity, alkalinity, and total dissolved As and As(III) concentrations were higher in the floodplain than in the channel to the west of New Island (Fig. 5). In groundwater, two zones with varying solute concentrations, a low conductivity fringe zone and a high conductivity center zone, have been previously described for island groundwater (Mladenov et al., 2008). At New Island there are also at least two distinct zones along the west–east transect; a lower conductivity, low As zone that stretches from the western island shore through the riparian zone of the island (approximately 60 m from the shoreline) and is characterized by low to moderate conductivity and pH and a high conductivity, high As zone with more elevated pH that is near the eastern shore (between 70 and 100 m from the western shore; Figs. 2 and 5) in a barren area colonized by the salt-tolerant spiky grass, *Sporobolus spikatus*. East of 105 m, no samples were collected. With the exception of samples collected at New 2 and from the termite mound, where some solute concentrations were high despite being close to shore, most solute concentrations were substantially lower in the low As zone than in the concentration zone.

In the concentration zone, the highest concentrations of most solutes were found (Table 1). Wells New 9, New 11, and New 12 contained the highest total As (between 87.5 and 186 $\mu g/L$), and slightly higher SO_4^{2-} concentrations (Table 1). Conductivity in this zone reached >6600 $\mu S/cm$ and pH ranged from 7.3 to 8.97 in 2 m depth wells. The termite mound, located approximately 101 m from edge of water but north of the sampled transect, also

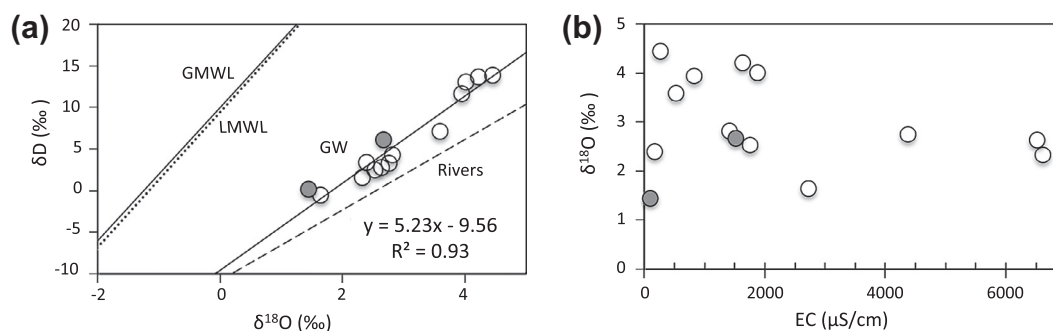


Fig. 4. Scatterplots of (a) deuterium (δD) and $\delta^{18}O$ for New Island groundwater (empty circles) and surface water (filled circles) with global meteoric water line (GMWL), local meteoric water line (LMWL; Mazor, 1977), and regional river water line (Mazor, 1977) included for comparison, and (b) $\delta^{18}O$ plotted against electrical conductivity (EC).

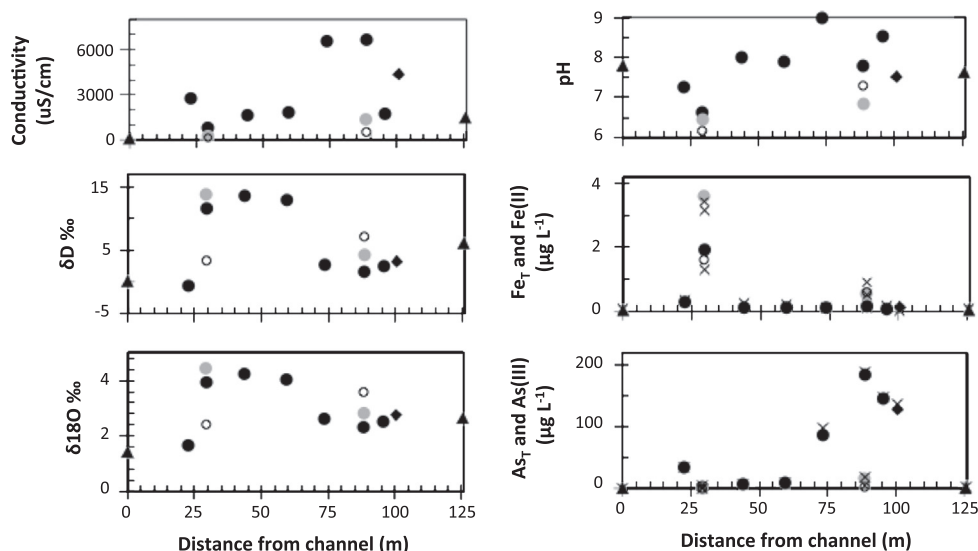


Fig. 5. Changes in groundwater solute chemistry (conductivity, stable isotopes of hydrogen and oxygen, pH, total Fe (Fe_T) and Fe(II), and total As (As_T) and As(III)) for surface water (triangle), termite mound groundwater (diamond), and groundwater collected at 2 m (black circle), 4 m (gray circle) and 6 m (unfilled circle) depths along the groundwater flowpath described in Fig. 2. An inverse longitudinal pattern exists between conductivity and stable isotopes of oxygen and hydrogen. Fe(II) and As(III) values are designated with an "x".

had high dissolved As concentration (138 μg As/L), fluoride (0.92 mg F/L), boron (1.01 mg B/L) and conductivity (4380 $\mu S/cm$) (Table 1; Fig. 5). New 2 also had high solute concentrations (Table 1). With the exception of groundwater at New 2, DOC concentrations increased along the groundwater flowpath and were higher in the concentration zone than elsewhere (Fig. 6). Concurrent with the DOC increase was a visible color loss in some groundwater samples that corresponded to lower SUVA values (Fig. 6).

For groundwater samples collected in the concentration zone, EEMs had lower amino acid-like fluorescence (ex/em of $\sim 275/300$ nm) and more intense humic-like (ex/em 240/450 nm) fluorescence (e.g. New 11 sample; Figs. 6 and 7) than surface water samples and samples collected from groundwater near the western shore (e.g. channel and New 7 samples; Figs. 6 and 7). The termite mound sample had more intense amino acid-like fluorescence and more resolved fulvic-like fluorescence (ex/em 320/430 nm) than groundwater samples collected in the concentration zone. In general, samples collected in the concentration zone had a higher HIX and lower freshness index (β/α ratio) than surface water samples and samples collected from groundwater underlying the riparian zone (Table 1). For groundwater samples, the FI and HIX were significantly and negatively correlated (Fig. 8). FI and β/α ratio were significantly and positively correlated (Fig. 8).

The deeper groundwater samples from 4 m and 6 m depths at New 3 and New 11 had lower pH, Eh, DOC, total As, and As(III) concentrations, lower HIX and SUVA values than samples collected at 2 m depths (Table 1, Fig. 6). Deeper groundwater samples collected at New 11 had substantially higher alkalinity and dissolved As concentrations and far lower dissolved Fe concentrations than those collected at 4 m and 6 m at New 3 (Table 1, Fig. 5). Active sulfate reducing bacteria were present in the 4 m and 6 m groundwater samples at New 3 and New 11, but only dead SRB cells were measured in the 2 m samples at both wells (Table 1).

Overlapping the shore and concentration zones, at approximately 60 m to 70 m from the western shore, is a zone of calcium- and magnesium-rich calcrite precipitation (calcrite zone) that is often visible at the soil surface in many islands. Application of concentrated HCl to the ground surface near New 7 resulted in bubbling and efflux of gas from the calcareous soil. Calcium and Mg concentrations were higher in the calcrite zone than in the concentration zone (Table 1). To evaluate the effects of evapoconcentration, we compared accumulation of solutes along the flowpath to that of the conservative ion, chloride (Cl), and found that accumulation rates differed (Table 2). Chloride concentration increased 35-fold, whereas DOC concentration increased only 5-fold and As increased 377-fold (Table 2).

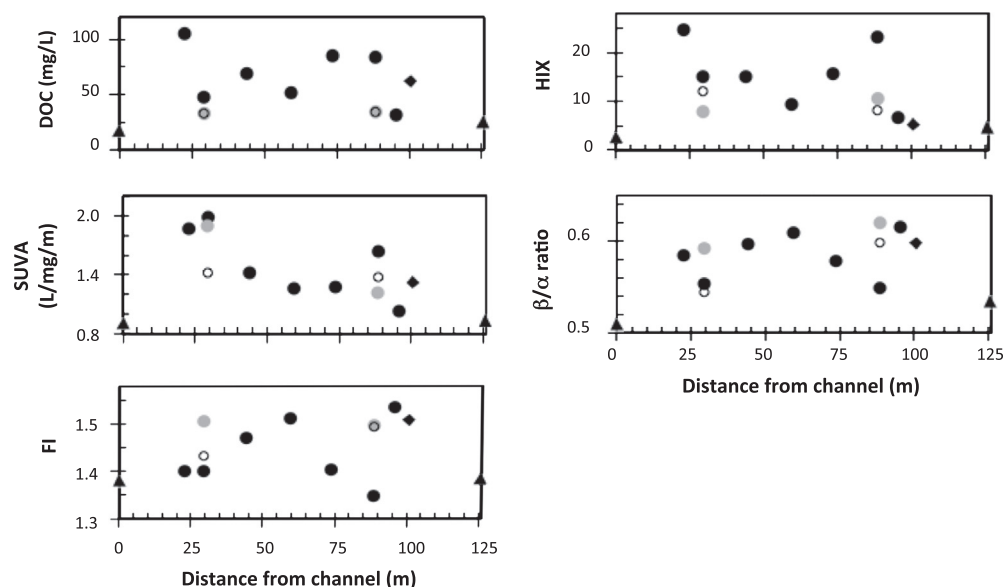


Fig. 6. Changes in groundwater DOM properties (DOC, SUVA, FI, HIX, and β/α ratio) for surface water (triangle), termite mound groundwater (diamond), and groundwater collected at 2 m (black circle), 4 m (gray circle) and 6 m (unfilled circle) depths along the groundwater flowpath described in Fig. 2.

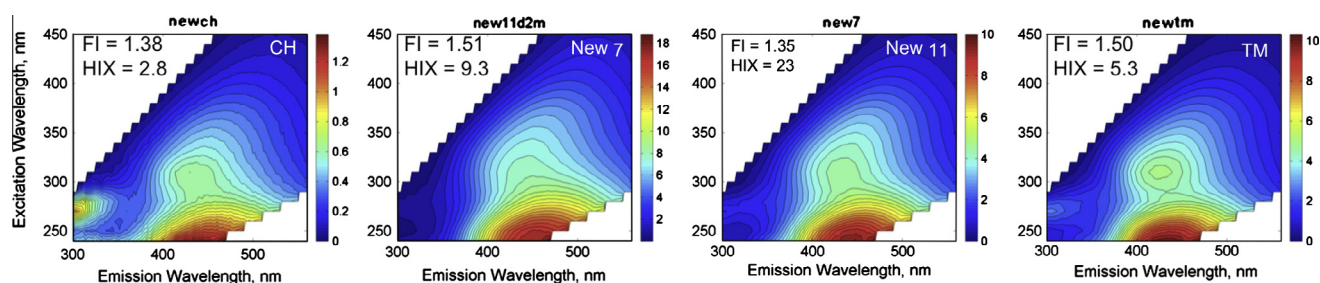


Fig. 7. Representative EEMs and corresponding fluorescence index (FI) and humification index (HIX) values of New Island groundwater samples from the channel (CH), New 7, New 11, and termite mound (TM).

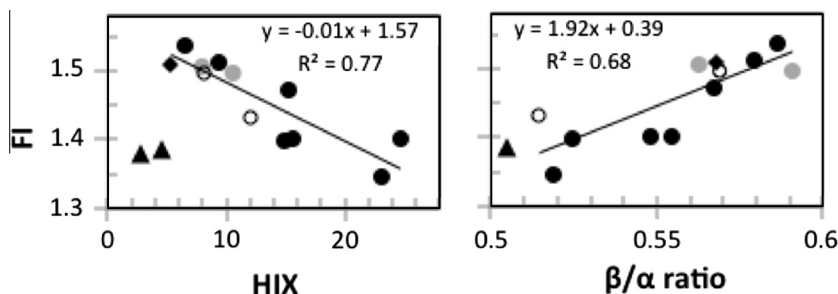


Fig. 8. Scatterplot of FI as a function of HIX and ratio for New Island groundwater at 2 m (black circle), 4 m (gray circle) and 6 m (unfilled circle) depths and at the termite mound (diamond). Surface water samples (triangles) are also shown but not included in linear regressions.

Bivariate correlations showed that significant relationships existed for total dissolved As and K, alkalinity, and conductivity (Table 3). Potassium concentration was also significantly related to conductivity and total alkalinity (Table 3). Dissolved organic carbon concentration was positively and significantly related to total S, Cl, and B concentrations, HIX, and UV_{254} (Table 3). The four principal components in the PCA accounted for 86.7% of the total variance. Factor 1 (48% of variance) was driven by HIX, B, DOC, Cl, NO_2 , NO_3 , SO_4 , and total S. Significant variables in factor 2 (21% of the variance) were EC, As, alkalinity, and K. Consistent with bivariate correlation results, factor analysis plots of PC1 and PC2 (Fig. 9) show that As was most highly correlated with EC, pH, alkalinity,

and K. In some environments elevated selenium can accompany high As, but Se was not detected in New Island groundwater (Table 1).

3.3. Sediment characterization

Surface soils at New 3 and New 11 had the highest content of TOC, N, and S (Table 4). Surface soil at New 3 and 2 m depth samples at New 11 had the highest As contents. Clay soils at 4 m depth at New 3 and 3.5 m depth at New 11 had the highest content of Fe, Al, and Si (Table 4). Linear combination fittings of XAS spectra (Fig. 9) showed As speciation in sediment at New 11, 2 m depth

Table 2
Ratio of groundwater:channel solute concentrations.*

Well or site	Distance from channel (m)	Cl ⁻	Total dissolved As	DOC	SO ₄ ²⁻	Alkalinity	Ca ²⁺
Channel	0	1.0	1.0	1.0	1.0	1.0	1.0
New2	22.7	85	66	5.8	24	–	8.9
New3	29.4	1.3	8.5	2.7	1.1	25	5.6
New5	43.9	5.9	12	3.9	1.4	40	8.5
New7	59.4	3.6	17	2.9	1.0	–	5.7
New9	73.5	33	194	4.7	1.6	130	1.4
New11	88.5	35	377	4.7	1.8	151	1.8
New12	95.6	1.6	297	1.8	1.0	45	3.1
Termite mound	100.6	32	276	3.5	5.2	–	5.5
Floodplain	125.6	1.1	2.4	1.4	1.0	7.3	1.8

* Dash indicates analyses were not performed due to insufficient sample volume.

Table 3
Bivariate correlations (R^2 value shown; number of samples in parentheses) and significance (* = p value < 0.05; ** = p value < 0.01; *** = p value < 0.001) for solutes and chemical characteristics in New Island groundwater. Only significant relationships are shown.

	Eh	pH	As	Fe	B DOC	HCO ₃ ⁻	Cl ⁻	NO ₂ ⁻	NO ₃ ⁻	SO ₄ ²⁻	Ca ²⁺	Na ⁺	K ⁺	S
Cond	0.66* (13)	0.65* (12)	0.79** (13)		0.74** (13)	0.99*** (10)	0.57* (13)						0.96*** (13)	0.59* (13)
Eh		0.66* (12)		-0.63* (13)	0.59* (13)	0.67* (10)							0.62* (13)	
pH			0.58* (12)	-0.77** (12)		0.68* (9)							0.63* (12)	
As						0.83** (11)							0.80** (14)	
Fe														
B					0.79** (14)		0.84*** (14)	0.74** (14)	0.77** (14)	0.77** (14)		0.78** (14)	0.62* (14)	0.77** (14)
DOC						0.89*** (11)	0.86*** (14)	0.60* (14)	0.61* (14)	0.63* (14)		0.75** (14)	0.76** (14)	0.91*** (14)
HCO ₃ ⁻							0.97*** (11)			0.62* (11)			0.98*** (11)	0.91*** (11)
F ⁻														
Cl ⁻								0.76* (14)	0.82*** (14)	0.89*** (14)		0.79** (14)	0.64* (14)	0.94*** (14)
NO ₂ ⁻									0.87*** (14)	0.90*** (14)	0.59* (14)	0.74** (14)		0.73** (14)
NO ₃ ⁻										0.94*** (14)	0.69** (14)	0.76** (14)		0.73** (14)
SO ₄ ²⁻											0.57* (14)	0.83*** (14)		0.81** (14)
Ca ²⁺												0.69** (14)		
Na ⁺														0.82*** (14)
K ⁺														0.60* (14)

contained orpiment-like (As₂S₃) and As(III)-like phases at 76% and 24%, respectively (Table 5). No pyrite or Fe–As phases were selected. In termite mound sediment, the linear combination fitting selected As(III) oxide and As(V) sorbed to ferrihydrite (Table 5).

4. Discussion

4.1. Hydrologic influence on groundwater As concentration

The spatial occurrence of high arsenic appears to be largely controlled by hydrologic and ecohydrologic processes in the groundwater of New Island. At distant Camp Island, [Huntsman-Mapila et al. \(2011\)](#) measured the highest groundwater As concentrations in the concentration zone underlying the island center. At New Island, we also measured highest As concentrations in a concentration zone characterized by barren sandy soil with salt-tolerant grass species at the surface, which, in contrast to Camp Island, is located close to the eastern shoreline. We hypothesize that the

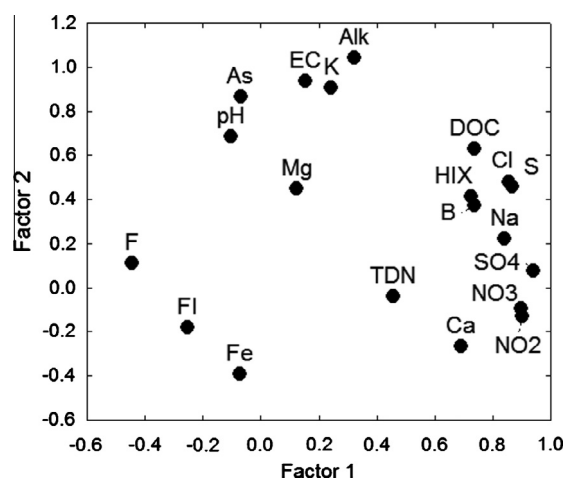


Fig. 9. PCA plot of factor 1 and 2 loadings using 20 New Island water chemistry variables in the analysis.

Table 4

Description of soil type, amounts of carbon (C) and nitrogen (N) and major elements, and cation exchange capacity (CEC) for sediment samples collected at various depths at New 3, New 11, termite mound (TM), and Boro channel muck.

Site	Depth (m)	Soil type	Total C (%)	TOC (%)	TIC (%)	Total N (%)	C:N	Al (g/kg)	Si (mg/kg)	S (mg/kg)	Mn (mg/kg)	Fe (mg/kg)	As (µg/kg)	CEC (meq/100 g)
New 3	0	Organic sand	3	2.4	0.57	0.21	11.7	5.1	<D. L.	264	142	2945	1290	12.5
	2	Dark sand	0.16	0.15	0.01	0.02	9.3	2.4	9.4	25.1	21.9	3111	772	2.9
	4	Clay	0.16	0.16	0	0.02	8.2	13.8	52.5	21.1	28.3	7333	373	10.7
	6	White sand	0.11	0.12	-0.01	0.02	6.2	1.2	13.6	10.4	0	635	0	1.5
New 11	0	Sand	0.4	0.26	0.14	0.05	5.7	16.6	41.2	31.7	116	3041	451	5.8
	2	Clayey sand	0.28	0.14	0.14	0.02	8.9	3.4	36	19.3	77.7	3842	1598	4.5
	3.5	Black clay	0.22	0.20	0.01	0.05	4	16.6	33.2	18.3	34.6	7418	542	11.8
	4	Beige sand	0.12	0.12	0	0.01	9.1	1.7	41.5	10.7	0	880	94	1.8
	6	White sand	0.11	0.11	0	0.01	19.3	0.5	53.6	10.9	0	352	0	0.8
	TM	3	Clay	1.2	0.35	0.81	0.04	8.8	7.9	13.6	242	180	4262	1690
Boro muck	-	Muck	9.1	7.5	1.6	0.8	9.2	16.1	19.1	618	191	7329	904	24.2

Table 5

Arsenic K-XANES fitting results for two samples performed in normalized space with an energy range from 11,860 to 11,930 eV showing percentage (%) of As compounds indicated by best fit.

Sample	Orpiment	As(III) oxide	Sorbed As(V)	Red. χ^2 ^a
New 11, 2 m depth	76.2	23.8	-	0.012
Termite mound	-	52.4	47.6	5.72

^a $\chi^2 = \sum(\text{fit} - \text{data})/\varepsilon^2 / (N_{\text{data}} - N_{\text{components}})$ is the reduced chi-square statistic. Here, ε is the estimated uncertainty in the normalized XANES data (taken as 0.01 for all data). The sum is over N_{data} points (77 data points between $E = 11,860$ and $11,930$ eV for all data), and $N_{\text{components}}$ is the number of components in the fit (either 2 or 3 as indicated in this table). The total percentage was constrained to be 100% in all fits. Typical uncertainties in the percentages listed for each standard component are < 10%. Dash indicates that the phase was not present.

shifting of the concentration zone to the east of center is a consequence of two-phase groundwater flow, dominated by asymmetric concentric flow during dry periods and through-flow during high flood (Fig. 3), driven by the higher surface water elevation of the western channel than the eastern floodplain (Fig. 2). Groundwater in the Okavango Delta is characterized by a Na/K-bicarbonate system (Huntsman-Mapila et al., 2011), and high concentrations of K and alkalinity in the concentration zone reflect the influence of evaporative concentration on dissolved solutes in groundwater. Also, the finding that all solutes are more concentrated at 2 m than at 4 m or 6 m depths confirms the conceptual models of previous studies (McCarthy et al., 1993; McCarthy, 2006, and references therein; Milzow et al., 2009) and further illustrates the importance of evapotranspiration for accumulating solutes near the water table. Significant bivariate correlations between As, conductivity, chloride, K, and alkalinity, supported by the results of PCA, suggest that evapoconcentration is also a major control on dissolved As, and probably dictates where high groundwater As concentrations can be expected on other islands of the Okavango.

The influence of evapoconcentration on solute accumulation is well-documented for groundwater of the Okavango Delta (McCarthy, 2006; Wolski et al., 2005). At New Island, the strong evaporative influence is also reflected in the stable isotopic signatures of oxygen and deuterium (Fig. 4). The deviation of our isotopic values from the global meteoric water line (GMWL) is due to evaporation (Gat, 1996). When evaporation from within the soil occurs during dry periods, isotopic fractionation and resulting isotopic enrichment can be seen in the remaining groundwater. During the rainy season the enriched waters can then be flushed downward and im-

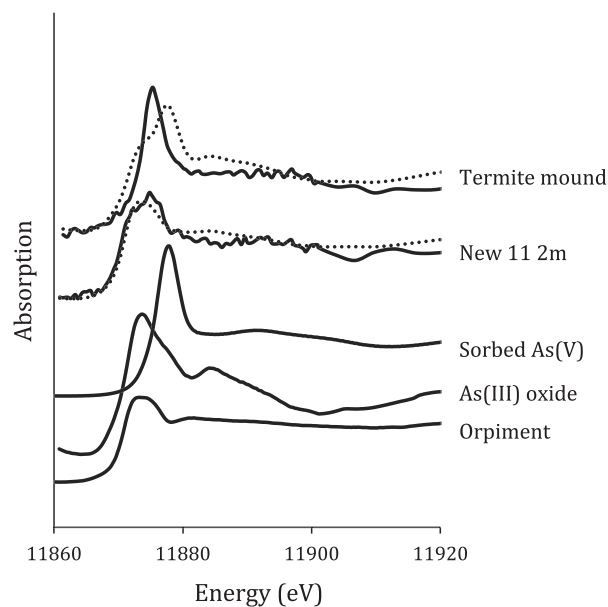


Fig. 10. Arsenic K-edge XANES spectra of samples and selected As standards used for linear combination fitting. Dotted lines indicate the linear combination XANES fits using selected As standards to represent various oxidation states of As.

part their evaporative isotope signature to the deeper groundwater.

Although hydrology is a predictor of where the highest As concentrations may be found, the controls on arsenic mobility are also biological and chemical. Evidence from conservative tracers (described later) suggests that additional processes besides evapoconcentration affect As mobility. In the next sections, we evaluate processes, illustrated in Fig. 11, that may lead to As sequestration and mobilization along the flowpath based on the groundwater and sediment chemistry results for the low As zone, concentration zone, and calcrete zone.

4.2. Low As zone processes

In the low As zone, active microbial processes influence both DOM and trace element chemistry. The high groundwater DOC concentrations, ranging from 32 to 104 mg/L in the 2 m depth

wells, reflect the influx of DOM-rich wetland surface water that occurs during the flood season (Mladenov et al., 2005, 2007). The lack of a steep increase in DOC concentration compared to the high accumulation rate of chloride (Table 2), suggests that DOM was consumed, presumably by microbial activity, and/or abiotically removed from solution. It is important to recognize that labile dissolved organic matter serves as an electron donor and, in wetland environments, high DOC concentrations help maintain reducing conditions and the dominance of reduced metal species (Chin et al., 1998). At New Island, both Fe and As were found predominantly in the reduced form. Microbially-reduced humic substances may also influence Fe and As speciation by directly reducing Fe and As or indirectly by acting as electron shuttles to accelerate the microbial reduction of Fe and As (Nevin and Lovley, 2000; Jiang and Kappler, 2008; Jiang et al., 2009; Mladenov et al., 2010). Humic substances in low-sulfate reducing environments have also been implicated in sulfur recycling to regenerate depleted sulfate and promote sulfate reduction (Blodau et al., 2007).

Other properties that influence DOM quality along the groundwater flowpath are pH and ionic strength. As the pH increases, the sorption of humic and fulvic acids to sediments becomes less favorable (Stumm and Morgan, 1996), so it is unlikely that increasing pH resulted in DOM sorption along the flowpath. Increasing ionic strength, on the other hand, substantially influences the structure of humic DOM, which is a major fraction of the total DOM pool (Mladenov et al., 2008), resulting in a more compact configuration that sorbs more readily to soil surfaces (Shen, 1999). Preferential sorption of humic DOM with increasing ionic strength may therefore also contribute to the less humic DOM (lower HIX) at New 5 and New 7.

In terms of inorganic constituents, the near-neutral pH and low alkalinity resulted in higher dissolved Fe concentrations at New 3 than in the concentration zone. As pH and bicarbonate concentrations increased with distance from the western shore, Fe was removed from solution (Table 1). This removal is consistent with the precipitation of Fe-carbonate that is geochemically predicted to occur under higher Eh and pH (Stumm and Morgan, 1996). Huntsman-Mapila et al. (2011) also observed a decrease in dissolved Fe along the groundwater flowpath of nearby Camp Island, which they attributed to precipitation reactions at higher pH.

In the low As zone from New 3 to New 7, total As and As(III) concentrations increased at more or less the same rate as chloride ion (Table 2). This pattern would suggest that either there are no sources or sinks for As along the flowpath or As mobilization is balanced by As precipitation. For New 11, located further down

the flowpath, X-ray absorption near-edge structure (XANES) spectroscopy analysis of sediment samples suggested that As precipitates with sulfide (discussed later; Fig. 10). Since there was not sufficient sample to perform XANES on sediment from the low As zone, the precipitation of As or its association with sulfides or Fe oxyhydroxides is not known for this site. Nevertheless, As(III) precipitation with sulfide or sulfhydryl groups may occur as a result of dissimilatory sulfate reduction by SRBs (Fig. 11). Our preliminary MPN measurements support the presence of SRBs in groundwater at New 3 and New 11. Although MPN values of groundwater samples (Table 1) were within the range measured in groundwater with high Fe–sulfide production (van Beek and van der Kooij, 1982), we expect that the sediments harbor greater microbial populations. Compared to chloride accumulation along the flowpath, sulfate accumulation is much lower, which would suggest that sulfate reduction is underway. At New Island, sulfate is also found in lower concentrations in the low As zone than in the concentration zone, which is consistent with the findings of Huntsman-Mapila (2011) for Camp Island.

Another important characteristic of the low As zone of New Island is that despite the very high DOC concentrations in the groundwater, the sandy sediments at New 3 or New 11 did not have visible peat or high TOC content (Table 4). Nor did the sediments have high As concentration (ranging from 0–1.7 mg kg⁻¹; Table 4), compared to the global average for soils of ~5 mg kg⁻¹ (Mandal and Suzuki, 2002). A recent study on humic-As associations in peat demonstrated that As(III) can be removed from solution by binding covalently to sulfhydryl groups in peat humic acids (Langner et al., 2011). The low sediment TOC and As content, however, suggests that sequestration of As by sediment organic matter is not a major pathway for arsenic removal in the groundwater at New Island. Nevertheless, it is important to note that the vegetation of New Island may be accumulating As from the groundwater. The surface soils at New 3 had the highest As and TOC concentration (Table 4), which may result from deposition of As-enriched plant matter or detritus in the organic surface soil horizon. Higher arsenic content (~900 µg/kg) was also measured in an organic muck sample collected from the sandy bottom of Boro side channel, which may reflect As-containing particulate organic matter derived from vegetation.

4.3. As mobilization in the concentration zone

As described earlier, there is indeed a significant and positive correlation between As and conductivity (Table 3), which would suggest that evapoconcentration is an important driver of high As concentration. However, compared to chloride as a conservative tracer, the accumulation of As in the concentration zone is between 5 (at New 9) and 80 (at New 12) times higher than that of Cl (Table 2), which would suggest that other mechanisms also contribute to As mobility.

Huntsman-Mapila et al. (2011) postulated that elevated groundwater As concentrations at nearby Camp Island could result from a combination of several processes: (1) evapoconcentration, (2) reductive dissolution of Fe oxyhydroxides, masked by reprecipitation, and (3) competitive interaction between HCO₃⁻ and As for the same sorption sites as pH increases. In an earlier study, Huntsman-Mapila et al. (2006) found that sediment As was positively and significantly correlated with sediment Fe. In our study, sediments collected from 2 m depth are primarily aluminum and iron minerals. Therefore, sorption of As to Fe oxides or oxyhydroxides, as is the case in reducing groundwater environments, such as those of the Bengal Basin (Mukherjee and Bhattacharya, 2001), may be possible. Despite this, at New 11, XANES analyses indicated that arsenic was not sorbed to ferric oxyhydroxides. Instead, solid-phase arsenic was present mainly as orpiment (As₂S₃; 76%) or

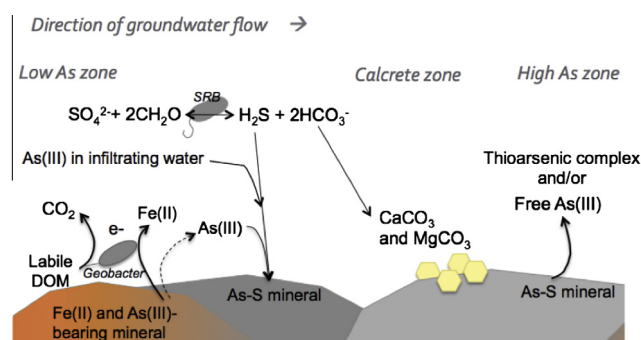


Fig. 11. Proposed reactions in groundwater of New Island. In the low As groundwater, reductive dissolution of Fe minerals may mobilize As, and sulfate reduction and generation of H₂S may simultaneously act to sequester As. CH₂O represents labile DOM. In the calcrete zone, bicarbonate reacts with Ca and Mg to form calcrete. In the high arsenic zone (concentration zone), As may be mobilized by As–S mineral dissolution at high pH or Eh and form thioarsenic complexes with sulfur. Evapoconcentration effects not shown.

As(III) oxide (24%), and no pyrite or other Fe–As phases were present. The occurrence of orpiment supports the notion that arsenic precipitates with sulfide in the concentration zone rather than with Fe (Fig. 10). Nevertheless, the possibility remains that in earlier segments of the groundwater flowpath (i.e., in the low As zone) As may be sorbed to Fe minerals. Also, we do not expect arsenite to sorb to calcite minerals because the sorption of As(III) on calcite is much less favorable than the sorption of As(V) (Sø et al., 2008), which was present in very low amounts in our study (Table 4).

In the deeper sediments and groundwater at New 3 and New 11 (at 4 m and 6 m depths) there is very little dissolved As or sediment As, or it is entirely absent. Sediment Fe content is also very low at the 6 m depth and is instead high where Al and Si are highest in the high CEC clay layers at 4 m depth in New 3 and at 3.5 m depth in New 11. These observations may suggest that when the older dune sands of the Okavango Delta were deposited (>100 kA; Ringrose et al., 2008) As was not present or not associated with Fe (oxy)hydroxides or other minerals. Instead, its presence in the Delta may be related to the annual deposition of clastic sediment derived from Angolan headwaters and more recent growth and formation of islands.

In the concentration zone there is evidence that the third process postulated by Huntsman-Mapila et al. (2011), a shift in competitive interactions at higher pH, does have an influence on arsenic mobility (Fig. 11). The solubility of As(III) in orpiment is greatly enhanced at higher pH (Newman et al., 1997; Kirk et al., 2010). If As(III) were adsorbed to other minerals its sorption would instead be higher at pH between 8 and 9 (Wang and Mulligan, 2006). At high pH and under sulfidic and reducing conditions, it was demonstrated that the dissolution of orpiment was followed by the formation of thioarsenate complexes that maintained As in solution (Suess and Planer-Friedrich, 2013). With similar ingredients present in the groundwater of Okavango Delta islands, it would be worthwhile to measure thioarsenate in the concentration zones of these waters.

Finally, desorption of As may also result from competition by humic substances for sorption sites or complexation of DOM with As, either directly or indirectly via bridging mechanisms with Ca²⁺ and Mg²⁺ cations (Wang and Mulligan, 2006, and references therein). Langner et al. (2011) also suggests that high groundwater DOM may enhance the mobility of As via complexation reactions. In a column study evaluating the formation of thioarsenic species in the presence of humic acid, humics did not contribute measurably to complexation reactions (Burton et al., 2013). However, sulfur–arsenic–humics complex formation has not been evaluated in natural systems. Given the high DOC concentrations at New 11 and the higher SUVA and HIX, which reflect more recalcitrant, aromatic, and humic DOM than in the low As zone, complexation with DOM must also be considered. It is also important to note that groundwater is a major sink for DOC in this recharge wetland (Mladenov et al., 2007), and taken together with the high DOC concentrations measured previously at Camp Island (Mladenov et al., 2008) and now at New Island, the low HIX and β/α ratio values of DOM in the concentration zone are evidence of potential sequestration of aged and humified DOM in groundwater throughout the Okavango Delta.

Interestingly, the termite mound groundwater also had high dissolved As concentration (Table 1), which was accompanied by high conductivity and elevated concentrations of other solutes, including DOC, F, Cl, and N and S species. Mounds built by *Macrotermes michaelseni* in the Okavango (Dangerfield et al., 1998) may be capable of active transport of water by capillary action (wicking) toward the mound to maintain moist conditions in the soil of the mound. Although the hydraulic processes that are responsible for maintaining soil water in termite mounds are still in question (Turner et al., 2006), the accumulation of solutes in the groundwater beneath mounds may be a consequence of such localized water movement

and subsequent evaporation from these zones. The high sediment As and TOC content of termite mound soil may result from translocation of As-enriched vegetation to the termite mound by the insects themselves. Indeed, the co-occurrence of active termite populations and comparatively high As sediment and groundwater concentrations is unexpected and warrants further investigation. The occurrence of high solute concentrations at New 2, in the early part of the flowpath, is also not well understood and merits further study.

4.4. Calcrete zone processes

In the calcrete zone between New 7 and New 9, the sharp decrease in Ca²⁺ and Mg²⁺ is consistent with the expected precipitation of these two cations as alkalinity and pH increases (Fig. 11). At the 2 m depths between New 5 and New 12, groundwater was saturated in calcite and dolomite (Table 1), which is consistent with PHREEQC modeling of saturation indices in groundwater of a larger island (Huntsman-Mapila et al., 2011). In the Okavango, subsurface precipitation of calcite and silica results in island expansion (McCarthy et al., 1993, 1998). In New Island groundwater, alkalinity progressively increased along the groundwater flowpath, in part as a result of evaporative concentration. In the initial segment of the groundwater flowpath (e.g. at New 2 and New 5) the GW:SW ratio for bicarbonate is 7–20 times higher than the GW:SW ratio of chloride, which suggests that bicarbonate also accumulates in solution as a result of calcium- and magnesium–carbonate dissolution and CO₂ generation by microbial oxidation of DOM. Indeed, the infiltration of DOM-rich surface water is a major pathway for DOM loss from floodplains (Mladenov et al., 2007), and the degradation of this fresh DOM input would be expected to add substantial amounts of bicarbonate to the groundwater.

An important terminal electron accepting process for New Island groundwater in general and for the calcrete zone in particular is sulfate reduction. In laboratory studies, SRBs were found to induce the precipitation of carbonate minerals by producing low molecular weight exopolymeric organic substances (EPS). EPS have a strong calcium-binding capacity that can induce calcite nucleation (Braisant et al., 2007) and may contribute to calcrete formation at New 7. In addition, SRBs are able to biodegrade high molecular weight lignin molecules into lower molecular weight depolymerized lignin byproducts in the presence of cellulosic compounds (Ko et al., 2009), which may contribute to the less aromatic nature of DOM in this zone. Finally, not only is sulfate reduction and the generation of hydrogen sulfide important for orpiment formation, but sulfate reducers can outcompete methanogens for electron donors and also oxidize methane that forms, thereby reducing the flux of methane to the atmosphere (Pester et al., 2012).

4.5. Dilution and dissolution by recent floods

The influence of the large floods of 2010–2011 is important to consider when interpreting how solutes are mobilized, sequestered, concentrated, and diluted in this groundwater system. Studies conducted at New Island prior to the large floods (Bauer-Gottwein et al., 2007; Ramberg and Wolski, 2008) reported much higher concentrations of most solutes in groundwater compared to those that we measured in 2011. The dilution effect caused by the influx of low conductivity surface water during the large floods of 2010–2011 can be evaluated by examining conservative solute concentrations. For example, chloride and bromide measured at New 11 were diluted at similar levels, 22-fold and 15-fold, respectively, from their 2003 concentrations (Table 6). To account for this dilution effect, the ratio of Pre/Post solute concentrations was normalized to the average of Pre/Post ratios of Cl and Br (Table 6). Values >1 signify additional solute removal processes, such as sorption, consumption, and mineralization, and values <1 signify

Table 6
Comparison of chemical properties and solute concentrations in groundwater at New 11 before and after the large floods of 2010–2011 and proposed mechanisms that may have influenced these values.

Chemical constituent	2003 Pre-floods [*]	2011 Post-floods	Pre/post	Pre/post: avg(Cl,Br) ^{**}	Proposed mechanisms
Cond ($\mu\text{S}/\text{cm}$)	11,360	6610	1.7	0.09	Evapoconcentration, dilution, and dissolution
pH	8.53	7.80	1.1	–	Dilution and influx of lower pH water
Ca ²⁺ (mg/L)	7.50	16.3	0.5	0.03	Dissolution by raising the water table
Mg ²⁺ (mg/L)	3.95	25.6	0.2	0.01	Dissolution by raising the water table
Na ⁺ (mg/L)	2617	70.8	37	2.0	Dilution
K ⁺ (mg/L)	550	312	1.8	0.10	Desorption when Ca and Mg resorb.
SO ₄ ²⁻ (mg/L)	126	2.99	42	2.3	Dilution and sulfate reduction
Alkalinity as CaCO ₃ (mg/L)	6606	4520	1.5	0.08	Dissolution at lower pH and DOM oxidation
Cl ⁻ (mg/L)	857	39.5	22	1.20	Dilution
F ⁻ (mg/L)	1.12	0.17	6.6	0.36	Not known
Br ⁻ (mg/L)	16.8	1.15	15	0.80	Dilution
NO ₃ ⁻ (mg/L)	95.9	1.12	86	4.7	Dilution and nitrate reduction
PO ₄ ³⁻ (mg/L)	11.4	0.20	57	3.1	Dilution and sorption
DOC (mg/L)	1007	83.4	12	0.66	Dilution and DOM degradation or sorption to sediments

^{*} Values from well DOTN8 (Bauer-Gottwein et al., 2007).

^{**} Pre/post ratio for each solute normalized to the average of Cl⁻ and Br⁻ pre/post ratios.

processes that mobilized solutes, such as dissolution and desorption (Table 6).

Mineral dissolution is likely to have a profound influence on groundwater chemistry as a result of the rise of the water table. We hypothesize that the raised water table of recent high flood years resulted in the exposure of new mineral surfaces to water and mineral dissolution. Because the calcrete and concentration zones contain carbonate minerals, dissolution also leads to a rise in alkalinity. The substantially higher concentrations of both Ca and Mg that we measured in 2011 compared to those measured prior to the high floods (Table 6) further suggest that mineral dissolution of CaCO₃ and MgCO₃ minerals occurred. With the higher concentrations of the multi-valent cations, Ca and Mg, brought into solution from the newly flooded unsaturated zone, Ca and Mg resorption would be expected and would cause the more weakly sorbed monovalent K to desorb from the sediments. The additional ions brought into solution from dissolution result in increased conductivity that balances the dilution effect (Table 6). Additionally, the influx and degradation of fresh carbon in the groundwater during the rising flood would also be expected to generate substantial CO₂ that would drive up alkalinity in the system (Table 6). Like Ca and Mg, the ratio of Pre/Post F concentrations normalized to the average of Pre/Post ratios of Cl and Br (Table 6) was <1.0, which would suggest that after the high flood conditions F was more mobile than prior to the high floods.

Prior to the high floods of 2010 and 2011, the difference between sulfate concentrations in the shore and concentration zones was much more pronounced, with sulfate concentrations as high as 126 mg/L in the concentration zone (well DOT8) of New Island in 2004 (Bauer-Gottwein et al., 2007). Sulfate concentrations measured in 2011 were low at most locations along the transect. Therefore, we hypothesize that, in 2011 under the conditions that prevailed after large-scale floods, the decreased sulfate concentrations may mean that reducing conditions, sulfate reduction, and H₂S production were more extensive than in previous years, reaching also into the concentration zone. However, it is not known whether those conditions would result in higher or lower dissolved As concentrations. Although orpiment formation and sequestration of As would be expected, increased formation of thioarsenates, as observed upon dissolution of orpiment in laboratory studies (Suess and Planer-Friedrich, 2013), may have increased dissolved As concentrations in recent years. Dissolved As concentration was not measured at New Island prior to the high floods and it is not possible to evaluate how the floods influenced its mobility.

5. Conclusion

Wetlands are dynamic aquatic environments in terms of redox conditions and biological and chemical reactivity. At New Island, groundwater flow and ecohydrologic processes form a concentration zone at New 11 as well as a zone of elevated solute concentrations beneath the termite mound. These results suggest that elevated As may be found in concentration zones of other islands in the Okavango. Along the groundwater flowpath at New Island, the biogeochemical evidence suggests that there is a co-existence of several biogeochemical processes that sequester and mobilize arsenic and transform organic matter. In the low As zone, As may be sequestered in the sediments via precipitation of As with sulfide, potentially produced by sulfate-reducing bacteria fueled by labile carbon. In the calcrete zone, the rise in pH and bicarbonate results in the formation of Ca- and Mg-rich calcrete. Finally, in the concentration zone, we propose As–S mineral formation (as orpiment), mineral dissolution under higher pH, and formation of complexes to maintain arsenic in solution. Extensive floods of 2010 and 2011 also had an important influence on groundwater geochemistry in New Island by promoting dissolution of calcrete and potentially by extending sulfate reducing conditions.

This study provides important insights into the conditions that influence As mobility in arid-zone environments. Nevertheless, more remains to be understood about the role of microorganisms, sulfur, and DOM in this respect. For example, additional information about microbial communities and the mineral phases present along the groundwater flowpath is needed to better understand the extent of Fe and sulfate reduction as well as the role of humic substances in sulfate recycling, sorption reactions, and complexation reactions.

Our understanding of these processes is important for water management in the Okavango region, which is currently sparsely populated, but increasing in population. Groundwater quality will continue to be an important topic in this water scarce region. In the Cuvelai and Kwando-Linyanti systems of Namibia and the Barotse floodplains of the upper Zambezi, which have a similar hydrologic regime to the Okavango Delta and share its headwaters (Mazvimavi and Wolski, 2006), the groundwater geochemistry should also be investigated with particular attention paid to the occurrence of trace elements, such as arsenic. This study is also relevant for other large wetland systems, such as the Everglades, which contain tree islands that also accumulate groundwater solutes (Wetzel et al., 2010; Sullivan et al., 2012) or the San Joaquin

Delta, which contains As-laden, reducing sediments and undergoes evapoconcentration processes (Belitz et al., 2003; Gao et al., 2007). Finally the processes described here also have important implications for other environments such as constructed wetlands (Lizama et al., 2011), in which inherent wetland properties, such as sulfate reduction and sorption reactions, have been harnessed to treat wastewater, remove nutrients, and sequester metals and toxic compounds.

Acknowledgements

We gratefully acknowledge N. Lokae and K. Phorano for assistance in the field and R. Karna, C. Kupe, M. Gondwe and K. Thorego for laboratory assistance. We also thank Dr. M. Kirk for assistance with saturation indices and geochemical calculations. We are grateful to P. Huntsman-Mapila for extensive comments on the manuscript and insightful discussion on the topic of arsenic in the Okavango Delta. The authors acknowledge the US National Science Foundation, NSF-INT 1105289, NSF-INT 1237290, and Kansas State University International Incentive Grant and University Small Research Grant programs for financial support.

References

- Ahmed, K.M., Bhattacharya, P., Hasan, M.A., Akhter, S.H., Alam, S.M.M., Bhuyian, M.A.H., Imam, M.B., Khan, A.A., Sracek, O., 2004. Arsenic enrichment in groundwater of the alluvial aquifers in Bangladesh – an overview. *Appl. Geochem.* 19, 181–200.
- ASTM Standard D4412-84, 2009. Standard test methods for sulfate-reducing bacteria in water and water-formed deposits. ASTM International, West Conshohocken, PA, United States. <http://dx.doi.org/10.1520/D4412-84R09>. <<http://www.astm.org>>.
- Bakhtar, D., Bradford, G.R., Lund, L.J., 1989. Dissolution of soils and geological materials for simultaneous elemental analysis by inductive plasma optical emission spectrometry and atomic absorption spectrometry. *Analyst* 114, 901–909.
- Bauer, P., Supper, R., Zimmermann, S., Kinzelbach, W., 2006. Geoelectrical imaging of groundwater salinization in the Okavango Delta, Botswana. *J. Appl. Geophys.* 60, 126–141.
- Bauer-Gottwein, P., Langer, T., Prommer, H., Wolski, P., Kinzelbach, W., 2007. Okavango Delta islands: interaction between density-driven flow and geochemical reactions under evapo-concentration. *J. Hydrol.* 334, 389–405.
- Beak, D.G., Basta, N.T., Scheckel, K.G., Traina, S.J., 2006. Bioaccessibility of Arsenic(V) Bound to Ferrihydrite Using a Simulated Gastrointestinal System. *Environ. Sci. Technol.* 40 (4), 1364–1370.
- Belitz, K., Dubrovsky, N.M., Burow, K., Jurgens, B., Johnson, T., 2003. Framework for a Ground-water Quality Monitoring and Assessment Program for California. U.S. Geological Survey, Water-Resource Investigation Report 03-4166.
- Bethke, C.M., 2009. The Geochemist's Workbench: Champaign, IL, Aqueous Solutions, LLC.
- Blodau, C., Mayer, B., Peiffer, S., Moore, T.R., 2007. Support for an anaerobic sulfur cycle in two Canadian peatland soils. *J. Geophys. Res.* 112, 1–10.
- Braissant, O., Decho, A.W., Dupraz, C., Glunk, C., Przekop, K.M., Viischer, P.T., 2007. Exopolymeric substances of sulfate-reducing bacteria: interactions with calcium at alkaline pH and implication for formation of carbonate minerals. *Geobiology* 5, 401–411.
- Burton, E.D., Johnston, S.G., Planer-Friedrich, B., 2013. Coupling of arsenic mobility to sulfur transformations during microbial sulfate reduction in the presence and absence of humic acid. *Chem. Geol.* 343, 12–24.
- Chapman, H.D., 1965. Cation exchange capacity. In: Black, C.A. (Ed.), *Methods of Soil Analysis*. ASA, pp. 891–901.
- Chin, Y., Traina, S.J., Swank, C.R., 1998. Abundance and properties of dissolved organic matter in pore waters of a freshwater wetland. *Limnol. Oceanogr.* 43 (6), 1287–1296.
- Coble, P.G., 1996. Characterization of marine and terrestrial DOM in seawater using excitation–emission matrix spectroscopy. *Mar. Chem.* 51, 325–346.
- Dangerfield, J.M., McCarthy, T.S., Ellery, W.N., 1998. The mound-building termite *Macrotermes michaelseni* as an ecosystem engineer. *J. Trop. Ecol.* 14 (4), 507–520.
- Delany, J.M., Lundeen, S.R., 1990. The LLNL Thermochemical Database. Lawrence Livermore National Laboratory.
- Fendorf, S., Michael, H.A., Van Geen, A., 2010. Spatial and temporal variations of ground-water arsenic in south and south east Asia. *Science* 328, 1123–1127.
- Gao, S., Ryu, J., Tanji, K.K., Herbel, M.J., 2007. Arsenic speciation and accumulation in evapo concentrating waters of agricultural evaporation basins. *Chemosphere* 67, 862–871.
- Gat, J.R., 1996. Oxygen and hydrogen isotopes in the hydrologic cycle. *Ann. Rev. Earth Planet. Sci.* 24, 225–262.
- Gieske, A., 1996. Vegetation driven groundwater recharge below the Okavango Delta (Botswana) as a solute sink mechanism: an indicative model. *Bot. J. Earth. Sci.* 3, 33–37.
- Greenberg, A.E., Clesceri, L.S., Eaton, A.D., 1992. Phenanthroline method. In: *Standard Methods for the Examination of Water and Wastewater*, 18th ed. APHA, Washington, 3500-Fe D.
- Gumbrecht, T., McCarthy, J., McCarthy, T.S., 2004. Channels, wetlands and islands in the Okavango Delta, Botswana, and their relation to hydrological and sedimentological processes. *Earth. Surf. Proc. Land.* 29, 15–29.
- Helgeson, H.C., 1969. Thermodynamics of hydrothermal systems at elevated temperatures and pressures. *Am. J. Sci.* 267, 729–804.
- Huntsman-Mapila, P., Mapila, T., Letshwenyo, M., Wolski, P., Hemond, C., 2006. Characterization of arsenic occurrence in the water and sediments of the Okavango Delta, NW Botswana. *Appl. Geochem.* 8, 1376–1391.
- Huntsman-Mapila, P., Nsengimana, H., Torto, N., Diskin, S., 2011. Arsenic distribution and geochemistry in groundwater of a recharge wetland in NW Botswana. In: IYPE (Eds.), *Groundwater*. Springer.
- Impellitteri, C.A., 2004. Effects of pH and competing anions on the speciation of arsenic in fixed ionic strength solutions by solid phase extraction cartridges. *Water Res.* 38, 1207–1214.
- Izbicki, J.A., Stamos, C.L., Metzger, L.F., Halford, K.J., Kulp, T.R., Bennett, G.L., 2008. Source, Distribution, and Management of Arsenic in Water from Wells, Eastern San Joaquin Ground-Water Sub Basin, California. US Geological Survey Open File Report, 2008-1272.
- Jiang, J., Kappler, A., 2008. Kinetics of microbial and chemical reduction of humic substances: implications for electron shuttling. *Environ. Sci. Technol.* 42 (10), 3563–3569.
- Jiang, J., Bauer, I., Paul, A., Kappler, A., 2009. Arsenic redox changes by microbially and chemically formed semiquinone radicals and hydroquinones in a humic substance model quinone. *Environ. Sci. Technol.* 43 (10), 3639–3645.
- Kirk, M.F., Roden, E.E., Crossey, L.J., Brealey, A.J., Spilde, M.N., 2010. Experimental analysis of arsenic precipitation during microbial sulfate and iron reduction in model aquifer sediment reactors. *Geochim. Cosmochim. Acta* 74, 2538–2555.
- Ko, J.J., Shimizu, Y., Ikeda, K., Kim, S.K., Park, C.H., Matsui, S., 2009. Biodegradation of high molecular weight lignin under sulfate reducing conditions: lignin degradability and degradation by-products. *Bioresour. Technol.* 100 (4), 1622–1627.
- Langner, P., Mikutta, C., Kretzschmar, R., 2011. Arsenic sequestration by organic sulphur in peat. *Nat. Geosci.* 5, 66–73.
- Lizama, A., Fletcher, K., Sun, T.D., 2011. Removal processes for arsenic in constructed wetlands. *Chemosphere* 84, 1032–1043.
- Mandal, B.K., Suzuki, K.T., 2002. Arsenic round the world: a review. *Talanta* 58, 201–235.
- Mazor, E., Verhagen, B.T., Sellschop, J.P.F., Jones, M.T., Robins, N.E., Hutton, L., Jennings, C.M.H., 1977. Northern Kalahari ground- waters: hydrologic, isotopic and chemical studies at Orapa. Botswana. *J. Hydrol.* 34, 203–234.
- Mazvimavi, D., Wolski, P., 2006. Long-term variations of annual flows of the Okavango and Zambezi Rivers. *Phys. Chem. Earth, Parts A/B/C* 31 (15), 944–951.
- McArthur, J.M., Banerjee, D.M., Hudson-Edwards, K.A., Mishra, R., Purohit, R., Ravenscroft, P., Cronin, A., Howarth, R.J., Chatterjee, A., Talukder, T., Lowry, D., Houghton, S., Chadha, D.K., 2004. Natural organic matter in sedimentary basins and its relation to arsenic in anoxic ground water: the example of West Bengal and its worldwide implications. *Appl. Geochem.* 19, 1255–1293.
- McCarthy, T.S., Ellery, W.N., 1995. Sedimentation on the distal reaches of the Okavango Fan, Botswana, and its bearing on calcrete and silcrete (ganister) formation. *J. Sediment. Res.* 65, 77–90.
- McCarthy, T.S., Ellery, W.N., Ellery, K., 1993. Vegetation-induced subsurface precipitation of carbonate as an aggradational process in the permanent swamps of the Okavango (delta) fan, Botswana. *Chem. Geol.* 107, 111–131.
- McCarthy, T.S., Ellery, W.N., Dangerfield, J.M., 1998. The role of biota in the initiation and growth of islands on the floodplain of the Okavango alluvial fan, Botswana. *Earth Surf. Process. Landform.* 23 (4), 291–316.
- McCarthy, T.S., 2006. Groundwater in the wetlands of the Okavango Delta, Botswana, and its contribution to the structure and function of the ecosystem. *J. Hydrol.* 320, 264–282.
- McKnight, D.M., Boyer, E.W., Westerhoff, P.K., Doran, P.T., Kulbe, T., Andersen, A.T., 2001. Spectrofluorometric characterization of dissolved organic matter for indication of precursor organic material and aromaticity. *Limnol. Oceanogr.* 46, 38–48.
- Milzow, C., Kgotlhang, L., Bauer-Gottwein, P., Meier, P., Kinzelbach, W., 2009. Regional review: the hydrology of the Okavango Delta, Botswana—processes, data and modelling. *Hydrogeol. J.* 17 (6), 1297–1328.
- Mladenov, N., McKnight, D.M., Wolski, P., Ramberg, L., 2005. Effects of annual flooding on dissolved organic carbon dynamics within a pristine wetland, the Okavango delta, Botswana. *Wetlands* 25, 622–638.
- Mladenov, N., McKnight, D.M., Wolski, P., Murray-Hudson, M., 2007. Simulation of DOM fluxes in a seasonal floodplain of the Okavango delta, Botswana. *Ecol. Model.* 205, 181–195.
- Mladenov, N., Huntsman-Mapila, P., Wolski, P., Masamba, W.R.L., McKnight, D.M., 2008. Dissolved organic matter accumulation, reactivity, and redox state in ground water of a recharge wetland. *Wetlands* 28, 747–759.
- Mladenov, N., Zheng, Y., Miller, M.P., Nemergut, D.R., Legg, T., Simone, B., Hageman, C., Rahman, M.M., Ahmed, K.M., McKnight, D.M., 2010. Dissolved organic matter sources and consequences for iron and arsenic mobilization in Bangladesh aquifers. *Environ. Sci. Technol.* 44, 123–128.

- Mukherjee, A.B., Bhattacharya, P., 2001. Arsenic in groundwater in the Bengal Delta Plain: slow poisoning in Bangladesh. *Environ. Rev.* 9 (3), 189–220.
- Nevin, K.P., Lovley, D.R., 2000. Potential for nonenzymatic reduction of Fe(III) via electron shuttling in subsurface sediments. *Environ. Sci. Technol.* 34, 2472–2478.
- Newman, D.K., Beveridge, T.J., Morel, F., 1997. Precipitation of arsenic trisulfide by *Desulfotomaculum auripigmentum*. *Appl. Environ. Microb.* 63, 2022.
- Newville, M., 2001. Interactive EXAFS analysis and FEFF fitting. *J. Synchrotron Radiat.* 8, 322–324.
- Nordstrom, D.K., 2002. World wide occurrences of arsenic in ground water. *Science* 296, 2143–2145.
- Parlanti, E., Wörz, K., Geoffroy, L., Lamotte, M., 2000. Dissolved organic matter fluorescence spectroscopy as a tool to estimate biological activity in a coastal zone submitted to anthropogenic inputs. *Org. Geochem.* 31, 1765–1781.
- Pester, M., Knorr, K.H., Friedrich, M.W., Wagner, M., Loy, A., 2012. Sulfate-reducing microorganisms in wetlands—fameless actors in carbon cycling and climate change. *Front. Microbiol.* 3 (72), 1–19.
- Planer-Friedrich, B., London, J., McCleskey, R.B., Nordstrom, D.K., Wallschläger, D., 2007. Thioarsenates in geothermal waters of Yellowstone National Park – determination, preservation, and geochemical importance. *Environ. Sci. Technol.* 41, 5245–5251.
- Ramberg, L., Wolski, P., 2008. Growing islands and sinking solutes: processes maintaining the endorheic Okavango delta as a freshwater system. *Plant. Ecol.* 196, 215–238.
- Rango, T., Bianchini, G., Beccaluva, L., Tassinari, R., 2010. Geochemistry and water quality assessment of central Main Ethiopian Rift natural waters with emphasis on source and occurrence of fluoride and arsenic. *J. Afr. Earth Sc.* 57, 479–491.
- Ravenscroft, P., Brammer, H., Richards, K.S., 2009. Arsenic in South and Central America, Africa, Australasia and Oceania Arsenic Pollution a Global Synthesis, vol. 6. Wiley-Blackwell, pp. 16–18.
- Ringrose, S., Huntsman-Mapila, P., Downey, W., Coetzee, S., Fey, M., Vanderpost, C., Vink, B., Kemosidile, T., Kolokose, D., 2008. Diagenesis in Okavango fan and adjacent dune deposits with implications for the record of palaeo-environmental change in Makgadikgadi–Okavango–Zambezi basin, northern Botswana. *Geomorphology* 101 (4), 544–557.
- Ryu, J.H., Gao, S., Dahlgren, R.A., Zierenberg, R.A., 2002. Arsenic distribution, speciation and solubility in shallow groundwater of Owens Dry Lake, California. *Geochim. Cosmochim. Acta* 66 (17), 2981–2994.
- Ryu, J., Gao, S., Tanji, K.K., 2011. Accumulation and speciation of selenium in evaporation basins in California, USA. *J. Geochem. Exp.* 110, 216–224.
- Schreiber, M.E., Simo, J.A., Freiberg, P.G., 2000. Stratigraphic and geochemical controls on naturally occurring arsenic in groundwater, eastern Wisconsin USA. *Hydrogeol. J.* 8, 161–176.
- Shen, Y.H., 1999. Sorption of humic acid to soil: the role of soil mineral composition. *Chemosphere* 38 (11), 2489–2499.
- Smedley, P.L., Kinniburgh, D.G., 2002. A review of the source, behaviour and distribution of arsenic in natural waters. *Appl. Geochem.* 17, 517–568.
- Sø, H.U., Postma, D., Jakobsen, R., Larsen, F., 2008. Sorption and desorption of arsenate and arsenite on calcite. *Geochim. Cosmochim. Acta* 72 (24), 5871–5884.
- Strickland, T.C., Fitzgerald, J.W., Ash, J.T., Swank, W.T., 1987. Organic sulfur transformations and sulfur pool sizes in soil and litter from a southern Appalachian hardwood forest. *Soil Sci.* 143, 453–458.
- Stucker, V.K., Williams, K.H., Robbins, M.J., Ranville, J.F., 2013. Arsenic geochemistry in a biostimulated aquifer: an aqueous speciation study. *Environ. Toxicol. Chem.* 32 (6), 1216–1223.
- Stumm, Morgan, 1996. *Aquatic Chemistry: Chemical Equilibria and Rates in Natural Waters*. John Wiley and Sons, New York, NY.
- Suess, E., Planer-Friedrich, B., 2012. Thioarsenate formation upon dissolution of orpiment and arsenopyrite. *Chemosphere* 89 (11), 1390–1398.
- Sullivan, P.L., Price, R.M., Miralles-Wilhelm, F., Ross, M.S., Scinto, L.J., Dreschel, T.W., Sklar, F.H., Cline, E., 2012. The role of recharge and evapotranspiration as hydraulic drivers of ion concentrations in shallow groundwater on Everglades tree islands, Florida (USA). *Hydrol. Process.* 10, 75–95.
- Turner, J.S., 2006. Termites as mediators of the water economy of arid savanna ecosystems. *Dryland Ecohydrology*. Springer, Netherlands, pp. 303–313.
- van Beek, C.G.E.M., van der Kooij, D., 1982. Sulfate reducing bacteria in groundwater from clogging and nonclogging shallow wells in the Netherlands River Region. *Groundwater* 20 (3), 298–302.
- Wang, S., Mulligan, C.N., 2006. Effect of natural organic matter on arsenic release from soils and sediments into groundwater. *Environ. Geochem. Hlth.* 28, 197–214.
- Weishaar, J.L., Aiken, G.R., Bergamaschi, B.A., Fram, M.S., Fujii, R., Mopper, K., 2003. Evaluation of specific ultraviolet absorbance as an indicator of the chemical composition and reactivity of dissolved organic carbon. *Environ. Sci. Technol.* 37, 4702–4708.
- Welch, A.H., Westjohn, D.B., Helsel, D.R., Wanty, R.B., 2000. Arsenic in ground water of the United States: occurrence and geochemistry. *Ground Water* 38, 589–604.
- Wetzel, P.R., Sklar, F.H., Coronado, C.A., Troxler, T.G., Kruna, S.L., Sullivan, P.L., Ewe, S., Price, R.M., Newman, S., Orem, W.H., 2010. Biogeochemical processes on tree islands in the greater everglades: initiating a new paradigm, a critical review. *Environ. Sci. Technol.* 41, 670–701.
- Wolski, P., Savenije, H.H.G., 2006. Dynamics of floodplain-island groundwater flow in the Okavango Delta, Botswana. *J. Hydrol.* 320, 283–301.
- Wolski, P., Murray-Hudson, M., Fernkuist, P., Liden, A., Huntsman-Mapila, P., Ramberg, L., 2005. Islands in the Okavango Delta as sinks of water-borne nutrients. *Botswana Notes Rec.* 37, 253–263.
- Zimmermann, S., Bauer, P., Held, R., Walther, J., Kinzelbach, W., 2006. Salt transport on islands in the Okavango Delta. *Adv. Water Resour.* 29, 11–29.
- Zsolnay, A., Baigar, E., Jimenez, M., Steinweg, B., Saccomandi, F., 1999. Differentiating with fluorescence spectroscopy the sources of dissolved organic matter in soils subjected to drying. *Chemosphere* 38, 45–50.